

1 **Global scale evaluation of precipitation datasets for**  
2 **hydrological modelling**

3 Solomon H. Gebrechorkos<sup>1,2</sup>, Julian Leyland<sup>2</sup>, Simon J. Dadson<sup>1</sup>, Sagy Cohen<sup>3</sup>, Louise Slater<sup>1</sup>,  
4 Michel Wortmann<sup>1</sup>, Philip J. Ashworth<sup>4</sup>, Georgina L. Bennett<sup>5</sup>, Richard Boothroyd<sup>6</sup>, Hannah  
5 Cloke<sup>7,8</sup>, Pauline Delorme<sup>9</sup>, Helen Griffith<sup>7</sup>, Richard Hardy<sup>10</sup>, Laurence Hawker<sup>11</sup>, Stuart  
6 McLelland<sup>9</sup>, Jeffrey Neal<sup>11</sup>, Andrew Nicholas<sup>5</sup>, Andrew J. Tatem<sup>2</sup>, Ellie Vahidi<sup>5</sup>, Yinxue Liu<sup>1</sup>,  
7 Justin Sheffield<sup>2</sup>, Daniel R. Parsons<sup>10</sup>, Stephen E. Darby<sup>2</sup>

8 <sup>1</sup>School of Geography and the Environment, University of Oxford, Oxford, UK

9 <sup>2</sup>School of Geography and Environmental Science, University of Southampton, Southampton, SO17 1BJ, United  
10 Kingdom

11 <sup>3</sup>Department of Geography and the Environment, University of Alabama, Tuscaloosa, AL, USA

12 <sup>4</sup>School of Applied Sciences, University of Brighton, Sussex, BN2 4AT

13 <sup>5</sup>Department of Geography, Faculty of Environment, Science and Economy, University of Exeter, Exeter, EX4  
14 4RJ, United Kingdom

15 <sup>6</sup>School of Geographical & Earth Sciences, University of Glasgow, UK

16 <sup>7</sup>Department of Geography and Environmental Science, University of Reading, UK

17 <sup>8</sup>Department of Meteorology, University of Reading, UK

18 <sup>9</sup>Energy and Environment Institute, University of Hull, Hull, United Kingdom

19 <sup>10</sup>Department of Geography, Durham University, Lower Mountjoy, South Road, Durham, DH1 3LE

20 <sup>11</sup>School of Geographical Sciences, University of Bristol, Bristol, BS8 1SS, UK

21 *Correspondence to:* Solomon H. Gebrechorkos ([solomon.gebrechorkos@ouce.ox.ac.uk](mailto:solomon.gebrechorkos@ouce.ox.ac.uk))

22 **Abstract.** Precipitation is the most important driver of the hydrological cycle but is challenging to estimate over  
23 large scales from satellites and models. Here, we assessed the performance of six global and quasi-global high-  
24 resolution precipitation datasets (European Center for Medium-range Weather Forecast (ECMWF) Reanalysis  
25 version 5 (ERA5), Climate Hazards group Infrared Precipitation with Stations version 2.0 (CHIRPS), Multi-  
26 Source Weighted-Ensemble Precipitation version 2.80 (MSWEP), TerraClimate (TERRA), Climate Prediction  
27 Centre Unified version 1.0 (CPCU) and Precipitation Estimation from Remotely Sensed Information using  
28 Artificial Neural Networks-Cloud Classification System-Climate Data Record (PERCCDR)) for hydrological  
29 modelling globally and quasi-globally. We forced the WBMsed global hydrological model with the precipitation  
30 datasets to simulate river discharge from 1983 to 2019 and evaluated the predicted discharge against 1825  
31 hydrological stations worldwide, using a range of statistical methods. The results show large differences in the  
32 accuracy of discharge predictions when using different precipitation input datasets. Based on evaluation at annual,  
33 monthly and daily time scales, MSWEP followed by ERA5 demonstrated a higher correlation (CC) and Kling-  
34 Gupta Efficiency (KGE) than other datasets for more than 50% of the stations. Whilst ERA5 was the second-  
35 highest performing dataset and it showed the highest error and bias in about 20% of the stations. The PERCCDR  
36 is the least well-performing dataset with bias of up to 99% and a normalised root mean square error of up to 247%.  
37 PERCCDR only show a higher KGE and CC than the other products in less than 10% of the stations. Even though  
38 MSWEP provided the highest performance overall, our analysis reveals high spatial variability, meaning that it is  
39 important to consider other datasets in areas where MSWEP showed a lower performance. The results of this  
40 study provide guidance on the selection of precipitation datasets for modelling river discharge for a basin, region  
41 or climatic zone as there is no single best precipitation dataset globally. Finally, the large discrepancy in the  
42 performance of the datasets in different parts of the world highlights the need to improve global precipitation data  
43 products.

44  
45  
46  
47  
48  
49  
50  
51  
52  
53  
54  
55  
56

## 57 1. Introduction

58 Whilst precipitation is one of the most important components of the global hydrological cycle and regulates the  
59 climate system (Miao et al., 2019; Sadeghi et al., 2021), it remains one of the most challenging variables to  
60 estimate at a global scale using satellite data and modelling approaches (Michaelides et al., 2009; Kidd and  
61 Levizzani, 2011; Beck et al., 2017a; Ursulak and Coulibaly, 2021). Reliable precipitation data with sufficient  
62 spatial and temporal coverage and accurate representation of extreme events is crucial for various applications.  
63 These include the development of water resource management and planning strategies, hydrological applications  
64 including forecasting hydrological extremes, and climate change analysis (Mehran and AghaKouchak, 2014;  
65 Nguyen et al., 2018; Sadeghi et al., 2021; Acharya et al., 2019). Observed precipitation from meteorological  
66 stations is typically used at local to river basin scale with gauge-based gridded precipitation datasets, such as from  
67 the Global Historical Climatology Network (Menne et al., 2012), developed to study climate and hydrology over  
68 larger scales. However, precipitation from gauges and gauge-based gridded datasets have several drawbacks such  
69 as limited spatial and temporal coverage, prevalence of missing values, and limited accuracy in sparsely populated  
70 and remote areas (Kidd and Levizzani, 2011; Reichle et al., 2011; Kidd et al., 2017; Sun et al., 2018; Gebrechorkos  
71 et al., 2018; Hafizi and Sorman, 2022). In addition, data-sharing policies have caused significant challenges in  
72 obtaining data, particularly in developing countries (Gebrechorkos et al., 2018; Hafizi and Sorman, 2022).

73 Given the challenges in representing precipitation at global scales, satellite, climate model, and reanalysis-based  
74 precipitation datasets can form the basis for monitoring and prediction of water resources and hydrological  
75 extremes, particularly in data-scarce regions of the world (Sheffield et al., 2018; Dembélé et al., 2020).  
76 Nevertheless, uncertainties and errors in these datasets require careful analysis to assess their suitability for a  
77 specific use. Error in satellite-based precipitation estimates can be due to errors in the sensor measurements, the  
78 frequency of sampling, and the retrieval algorithms, including the representation of cloud physics (Dembélé et al.,  
79 2020; Laiti et al., 2018; Alazzy et al., 2017). Climate model-based datasets, including reanalyses, have large  
80 uncertainty due to their coarse spatial resolution and ambiguity associated with model parameters (Gebrechorkos  
81 et al., 2018; AL-Falahi et al., 2020; Dembélé et al., 2020; Her et al., 2019). Reanalysis datasets may correct for  
82 some of these errors via the assimilation of observational data, but this comes with its own uncertainties due to  
83 the error characteristics of the assimilated observations and the assimilation scheme (Sheffield et al., 2006; Parker,  
84 2016). In hydrological modelling, errors and biases in precipitation data result in poor representation of the  
85 hydrological responses and affect applications (Maggioni and Massari, 2018; Zambrano-Bigiarini et al., 2016).  
86 For example, according to Bárdossy et al. (2022), uncertainty in precipitation can lead to hydrological model  
87 errors of up to 50%. Hence, it is important to assess the quality and accuracy of the precipitation products before  
88 using them in global or basin-scale hydrological models. In data-limited regions, hydrological models driven by  
89 precipitation datasets developed from satellite sources, reanalysis or climate models are the only plausible way to  
90 represent the terrestrial water cycle (van Huijgevoort et al., 2013).

91 Over the last few decades, several global and quasi-global precipitation datasets have been developed that address  
92 some of these challenges and can be used to drive hydrological models at regional and global scales. These  
93 precipitation datasets differ in terms of their spatial resolution, spatial coverage (e.g., global or regional), data  
94 sources (e.g., gauge, satellite, reanalysis, and radar), temporal resolution (e.g., sub-daily and daily), and length of

95 record. It is therefore important to evaluate the accuracy of the datasets before they are used to drive global or  
96 regional scale hydrological models. Most studies have evaluated precipitation datasets using observed data from  
97 field-based meteorological stations at a range of scales (e.g., Beck et al., 2017a; Gebrechorkos et al., 2018; Xiang  
98 et al., 2021; Sun et al., 2018; Hong et al., 2022; Wati et al., 2022; AL-Falahi et al., 2020; Ahmed et al., 2019;  
99 Fallah et al., 2020). Hydrological models have also been used to assess the quality of the precipitation dataset by  
100 comparing simulated and observed discharge across different spatial scales (e.g., Mazzoleni et al., 2019; Beck et  
101 al., 2017a; Zhu et al., 2018; Raimonet et al., 2017; Guo et al., 2018; Wang et al., 2020; Salehi et al., 2022; Zhu et  
102 al., 2018; Seyyedi et al., 2015). In principle, this latter approach is able to identify the precipitation datasets which  
103 best represent hydrological variability including extremes, even in catchments where there have been multiple  
104 drivers of change.

105 There are a limited number of studies assessing multiple precipitation datasets for global hydrological model  
106 applications (Voisin et al., 2008; Beck et al., 2017a; Mazzoleni et al., 2019). Voisin et al. (2008) conducted a  
107 global-scale evaluation of two precipitation for hydrological modelling. Beck et al., (2017a) compared the  
108 performance of 22 precipitation datasets for global hydrological modelling. Mazzoleni et al. (2019) evaluated 18  
109 different precipitation datasets in eight river basins on different continents. Both Beck et al. (2017a) and Mazzoleni  
110 et al. (2019) found that merged satellite-observation precipitation products showed the best performance compared  
111 to satellite-only products. These studies exclusively concentrate on a daily time scale, evaluating performance  
112 solely through the Nash-Sutcliffe Efficiency (NSE). Neither study extends this assessment to monthly and annual  
113 time scales, and notably, they do not assess the hydrological extremes which are often considered important to  
114 capture. Here, we build upon the work by Beck et al., (2017a) by adding recently developed high-resolution  
115 precipitation datasets. These include the European Center for Medium-range Weather Forecast (ECMWF)  
116 Reanalysis version 5 (ERA5) (Hersbach et al., 2020), TerraClimate (Abatzoglou et al., 2018) and Precipitation  
117 Estimation from Remotely Sensed Information using Artificial Neural Networks-Cloud Classification System-  
118 Climate Data Record (PERCCDR, Sadeghi et al., 2021) and the latest Multi-Source Weighted-Ensemble  
119 Precipitation version 2.80 (MSWEP). These additions significantly broaden the scope of our study, offering a  
120 diverse range of products with distinct methodologies. In addition, we use multiple statistical metrics to evaluate  
121 the performance of the precipitation products for hydrological modelling at daily, monthly and annual time scales  
122 and for daily extremes, which represents a current gap in the modelling literature.

123 The aim of this study is to undertake a comprehensive evaluation, spanning various temporal and spatial scales,  
124 to examine how different input precipitation datasets impact the predictions of a global hydrological model. We  
125 assess six high-resolution precipitation datasets, each with records spanning over 30 years. A comprehensive and  
126 physically based gridded global hydrological model (WBMsed; Cohen et al., (2013)) is used to simulate river  
127 discharge globally. The model incorporates various datasets, including reservoirs, dams, and crop water  
128 requirements, which significantly influence streamflows. The objective is not to evaluate the absolute performance  
129 of the hydrological model, which can be influenced by local factors, rather our focus is on comparing the relative  
130 performance of the six precipitation datasets at individual locations. The modelled discharge, derived from the six  
131 precipitation datasets, is assessed across the various time scales by comparing it with observed discharge data  
132 collected from 1825 river gauge stations worldwide. Furthermore, we assess the performance of the precipitation  
133 products by examining their accuracy in representing daily extreme precipitation events across various percentiles.

134 In summary, this research offers a thorough evaluation of this set of diverse precipitation products, spanning from  
135 daily extreme events to annual time scales, providing an invaluable resource for selecting appropriate basin-to-  
136 regional-to-global scale inputs for hydrological modelling applications.

## 137 **2. Data and methods**

138 In the following sections, we outline the various input and evaluation datasets which were used within the  
139 WBMsed hydrological modelling framework. The statistical evaluation methods used to assess the results are also  
140 outlined.

### 141 **2.1. Precipitation datasets**

142 The precipitation datasets used herein are selected based on their length of record (>30 years period), spatial  
143 coverage (global and quasi-global) and recommendations from previous research (Beck et al., 2017a) (Table 1).  
144 Based on the findings of Beck et al. (2017a), datasets with low performance were excluded, while those  
145 demonstrating the highest performance, such as MSWEP and Climate Hazards group Infrared Precipitation with  
146 Stations version 2.0 (CHIRPS), were retained, and new datasets were incorporated. The selected precipitation  
147 datasets are the ERA5 ERA5, CHIRPS, MSWEP, TerraClimate (TERRA), Climate Prediction Centre Unified  
148 version 1.0 (CPCU), and PERCCDR. Due to their spatial coverage, CHIRPS and PERCCDR are evaluated only  
149 up to latitudes of 50°N and 60°N, respectively (Table 1). Each dataset was subsequently used to force the WBMsed  
150 hydrological model, to generate streamflow estimates. The availability of these datasets with longer records  
151 enables the assessment of long-term hydrological changes at global, regional, and catchment scales.

152 ERA5 is the fifth generation European Centre for Medium-Range Weather Forecasts (ECMWF) reanalysis data  
153 available globally from 1940 to present (Hersbach et al., 2020). ERA5 combines modelled data and observations  
154 to create a complete and consistent global climate dataset using advanced data assimilation methods. ERA5  
155 provides improved precipitation representation such as the inclusion of tropical cyclones when compared to the  
156 ERA-Interim (He et al., 2020; Jiao et al., 2021). In addition, ERA5-Land, a subset of ERA5 focusing on land  
157 areas, delivers more detailed climate information at higher spatial resolution (0.1°) from 1950 to the present  
158 compared to ERA5 (Hersbach et al., 2020). Here, ERA5-Land (referred to as ERA5) is used to evaluate its  
159 performance for global hydrological modelling. The data is freely available from Copernicus Climate Data Store  
160 (<https://cds.climate.copernicus.eu/cdsapp#!dataset/reanalysis-era5-land?tab=overview>).

161 CHIRPS is a high-resolution (0.05°) quasi-global rainfall product primarily developed for monitoring droughts  
162 and global environmental changes (Funk et al., 2015). CHIRPS provides coupled gauge-satellite precipitation  
163 estimates with a 0.05° spatial resolution and long-period records. The product is developed by combining satellite-  
164 only Climate Hazards group Infrared Precipitation (CHIRP), Climate Hazards group Precipitation climatology  
165 (CHPclim), and data from ground stations. CHIRP and CHPclim were developed based on calibrated infrared  
166 cold cloud duration (CCD) precipitation estimates and ground station data from the Global Historical Climate  
167 Network (GHCN). The product is available at the Climate Hazards Group (<https://www.chc.ucsb.edu/data/chirps/>)  
168 on daily, 10-day, and monthly timescales from the 1981-near present. Due to its availability at high spatial and  
169 temporal resolution, CHIRPS is widely used in hydrological studies (Luo et al., 2019; Gebrechorkos et al., 2020;

170 Geleta and Deressa, 2021; Wang et al., 2021; Opere et al., 2022; Day and Howarth, 2019; Gebrechorkos et al.,  
171 2019) and modelling of hydrological extremes such as droughts and floods (Chen et al., 2020; Mianabadi et al.,  
172 2022; Peng et al., 2020).

173 MSWEP is a global high-resolution ( $0.1^\circ$ ) precipitation product developed by merging multiple datasets such as  
174 ground stations (~77,000), satellite-based rainfall estimates, and reanalysis data (Beck et al., 2019b). MSWEP  
175 was developed by merging station data satellite datasets and reanalysis datasets (Beck et al., 2017b, 2019b).  
176 MSWEP has been widely used in regional and global scale hydrological studies such as for floods and droughts  
177 (Gu et al., 2023; Gebrechorkos et al., 2022b; Reis et al., 2022; Wu et al., 2018; Sun et al., 2022; Gebrechorkos et  
178 al., 2022c; Xiang et al., 2021; López López et al., 2017) and for developing high-resolution global scale  
179 hydrological extreme and climate datasets and regional drought monitoring (Gebrechorkos et al., 2023, 2022a; Li  
180 et al., 2022b). MSWEP is available from 1979-present at multiple timescales (e.g., 3 hourly) and can be accessed  
181 from the GloH2O website (<https://www.gloh2o.org/mswep/>).

182 TerraClimate (TERRA) is a high-resolution ( $0.04^\circ$ ) terrestrial monthly climate (e.g., precipitation and  
183 temperature) and climatic water-balance dataset available from 1958-2020 (Abatzoglou et al., 2018). TERRA was  
184 developed by combining high and coarse spatial resolution datasets such as WorldClim climatological normals  
185 and Climatic Research Unit gridded Time Series (CRU TS) and JRA-55, respectively. The data was evaluated  
186 against ground observation from the Historical Climate Network and exhibited better performance than the CRU-  
187 TS (Abatzoglou et al., 2018). The monthly climate and climatic water balance is available from the Climatology  
188 Lab website (<https://www.climatologylab.org/>).

189 CPCU is a gauge-based analysis of daily precipitation datasets available globally from 1979 to present at a spatial  
190 resolution of  $0.5^\circ$  (Chen et al., 2008). CPCU is the product of the CPC Unified Precipitation project at NOAA  
191 Climate Prediction Center. The product uses data from more than 30,000 (1979-2005) and 17,000 (2006-present)  
192 stations. The CPCU data is publicly available at the NOAA Physical Sciences Laboratory (PSL,  
193 [https://downloads.psl.noaa.gov/Datasets/cpc\\_global\\_precip/](https://downloads.psl.noaa.gov/Datasets/cpc_global_precip/)) and has been used for hydrological and climate  
194 studies (Beck et al., 2017a; Zhu et al., 2021; Hou et al., 2014).

195 The PERCCDR is a quasi-global (latitude from  $60^\circ\text{S}$  to  $60^\circ\text{N}$ ) dataset developed at the University of California  
196 (Sadeghi et al., 2021). PERCCDR provides precipitation estimates at high spatial ( $0.04^\circ$ ) and temporal (3-hourly)  
197 resolutions from 1983 to present. The dataset is developed using the rain rate output from the PERSIANN-CCS  
198 model, which uses GridSat-B1 IR and NOAA Climate Prediction Center (CPC-4km) IR data. Compared to other  
199 PERSIANN precipitation datasets, PERCCDR provides a realistic representation of precipitation extremes  
200 globally and shows better agreement with CPCU precipitation (Sadeghi et al., 2021). The PERCCDR has been  
201 used in hydrological studies (Salehi et al., 2022; Eini et al., 2022) and is freely available from the Center for  
202 Hydrometeorology and Remote Sensing (CHRS) Data Portal (<https://chrsdata.eng.uci.edu/>).

203 Table 1. The six precipitation datasets used in this study, their spatial and temporal resolution, spatial coverage  
204 and data sources.

Abbreviation	Full name	Spatial resolution and coverage	Temporal resolution	Temporal coverage	Data source	Reference
ERA5	ECMWF (European Centre for Medium-Range Weather Forecasts) Reanalysis V5	0.1°, global	Sub-daily	1979-present	Gauge and reanalysis	(Hersbach et al., 2020)
CHIRPS	Climate Hazards group Infrared Precipitation with Stations (CHIRPS) version 2.0	0.05°, quasi global (50°S-50°N)	Daily	1981-present	Gauge, satellite, and reanalysis	(Funk et al., 2015)
MSWEP	Multi-Source Weighted-Ensemble Precipitation (MSWEP) version 2.80	0.1°, global	Daily	1979-present	Gauge, satellite, and reanalysis	(Beck et al., 2019b)
TERRA	TerraClimate	0.042°, global	Monthly	1958-present	Gauge and reanalysis	(Abatzoglou et al., 2018)
CPCU	Climate Prediction Centre (CPC) Unified V1.0	0.5°, global	Daily	1979-present	Gauge only	(Chen et al., 2008)
PERCCDR	Precipitation Estimation from Remotely Sensed Information using Artificial Neural Networks-Cloud Classification System-Climate Data Record (PERSIANN-CCS-CDR)	0.04°, Quasi global (60°S-60°N)	Sub-daily	1983-present	Gauge and satellite	(Sadeghi et al., 2021)

## 205 2.2. WBMsed hydrological model

206 The WBMsed (Cohen et al., 2013, 2014) ~~hydrological~~ model is used to assess the performance of the different  
207 precipitation datasets for hydrological modelling globally. WBMsed is a global-scale hydrogeomorphic model,  
208 an extension of the WBMplus global hydrology model (Wisser et al., 2010), which is part of the FrAMES  
209 biogeochemical modelling framework (Wollheim et al., 2008). The WBMplus model is one of the first Global  
210 Hydrological Models (GHMs) applied to a global domain (Cohen et al., 2013; Grogan et al., 2022). The WBMsed  
211 model extends the WBMplus model by including sediment flux modules (suspended, bedload and suspended bed

212 ~~material; Cohen et al. 2022) & the WBMplus and BQART models. BQART, a global model, is specifically~~  
213 ~~employed for sediment flux modeling (Cohen et al., 2013, 2014). While we are not analyzing sediment flux in~~  
214 ~~this paper, we opted to use the WBMsed model for consistency with consequent analysis. The hydrological~~  
215 ~~prediction of WBMsed is equivalent to WBMplus.~~

216 The model represents the major hydrological cycle components of the land surface and tracks the balances and  
217 fluxes between the atmosphere, surface water storages, vegetation, runoff, and groundwater (Grogan et al., 2022).  
218 The model includes hydrological infrastructure (e.g., dams and reservoirs), agricultural water requirements, and  
219 domestic and industrial water uses. A gridded river network connects grid cells, which allows the routing of fluxes  
220 downstream (e.g., streamflow). The model requires several climate datasets as input in addition to precipitation,  
221 including temperature, humidity, air pressure, and wind speed (Table S1). Additional parameters such as field  
222 capacity, rooting depth, and riverbed slope are used to drive the model.

223 We use an identical model setup to that used by Cohen et al., (2022) with all input datasets as detailed in Cohen  
224 et al. (2013). Updates include daily ERA5 air temperature (Hersbach et al., 2020) re-gridded at 10 arc-minutes  
225 resolution, reservoir capacity from the global reservoir and dam database (GRanD v1.3; Lehner et al., (2011)),  
226 and a 6 arc-minute HydroSTN30 network derived from HydroSHEDS (Lehner et al., 2008). In addition, we used  
227 each of the six input precipitation datasets, ERA5, CHIRPS, MSWEP, TERRA, CPCU, and PERCCDR in turn,  
228 keeping all other parameters and inputs the same. All the input precipitation datasets are bilinearly interpolated to  
229 the same spatial resolution of 0.1°. Even though WBMsed can disaggregate monthly time series into daily,  
230 TERRA (only available at monthly resolution, see Table 1) is evaluated on monthly and annual time scales, whilst  
231 all other datasets are evaluated at daily, monthly and annual time scales. WBMsed simulations were run at 0.1°  
232 (~11km at the equator) spatial and daily and monthly temporal resolutions. Several WBMsed streamflow  
233 validation analyses have been reported previously (e.g., Cohen et al., 2022; Dunn et al., 2019; Cohen et al., 2014,  
234 2013; Moragoda and Cohen, 2020), which indicate that the model represents the long-term average observed  
235 streamflow globally. It is important to note that this study assesses the precipitation datasets without calibration  
236 of the WBMsed model for each precipitation dataset, which could theoretically improve their performance in  
237 replicating observed river discharge.

### 238 **2.3. Observed river discharge from ground stations**

239 Observed daily and monthly river discharge used to evaluate the hydrological model were obtained from the  
240 Global Runoff Data Centre (GRDC, 2023). The GRDC is an international data archive  
241 (<https://www.bafg.de/GRDC/>), which hosts data for over 10,000 hydrological stations. The number of stations  
242 with a length of record greater than 10 years during the evaluation period (1981-2019) are limited. Here, we  
243 consider stations with a minimum record length of 10 years, allowing for missing values within this period. Due  
244 to the spatial resolution of the input datasets and the model simulations (~11x11 km), we only consider stations  
245 with a catchment area of greater than 100 km<sup>2</sup>. Overall, 1825 suitable stations were identified with daily and  
246 monthly records, largely in North and South America, Europe and Australia, with very few stations in Africa and  
247 Asia (Figure 1).



248 **2.4. Evaluation metrics**

249 Several methods are used to assess the modelled discharge using the streamflow observations: the Pearson  
 250 correlation coefficient (CC, Eq. 1), Kling-Gupta Efficiency (KGE, Eq. 2) (Gupta et al., 2009), Root-Mean-Square  
 251 Error (RMSE, Eq.3) and Percentage of bias (Pbias, Eq.4). CC measures the linear relationship between observed  
 252 discharge and simulated discharge, focusing primarily on the degree of association between the two datasets. It is  
 253 particularly useful for assessing the strength and direction of this relationship, highlighting how well the model  
 254 captures the variability in discharge (Moazami et al., 2013). KGE is a comprehensive metric that evaluates the  
 255 overall agreement between observed and simulated streamflow, considering similarities in variability, amplitude,  
 256 and timing. It provides an assessment of the model's ability to capture both the magnitude and temporal dynamics  
 257 of the observed discharge (Gupta et al., 2009). RMSE measures the average magnitude of the differences between  
 258 observed and simulated discharge, providing a measure of the overall goodness of fit. Moreover, the percentage  
 259 of bias is used to quantify the systematic overestimation or underestimation of discharge by the model compared  
 260 to observations (Moazami et al., 2013). A KGE value of 1.0 indicates a perfect match between the observed and  
 261 simulated discharge, whereas values lower than -0.41 show that the model is worse than using the mean of the  
 262 observed discharge as a predictor (Knoben et al., 2019). For spatial comparison, the RMSE is normalised by the  
 263 standard deviation of the observed data (NRMSE; Eq. 5).

264 
$$CC = \frac{\sum_{i=1}^N (M_i - \bar{M}) * (O_i - \bar{O})}{\sqrt{\sum_{i=1}^N (M_i - \bar{M})^2} * \sqrt{\sum_{i=1}^N (O_i - \bar{O})^2}} \quad (1)$$

265 
$$KGE = 1 - \sqrt{(r - 1)^2 + (\alpha - 1)^2 + (\beta - 1)^2} \quad (2)$$

266 
$$RMSE = \sqrt{\frac{\sum_{i=1}^N (O_i - M_i)^2}{N}} \quad (3)$$

267 
$$Pbias = \frac{\sum_{i=1}^N (M_i - O_i)}{\sum_{i=1}^N O_i} * 100 \quad (4)$$

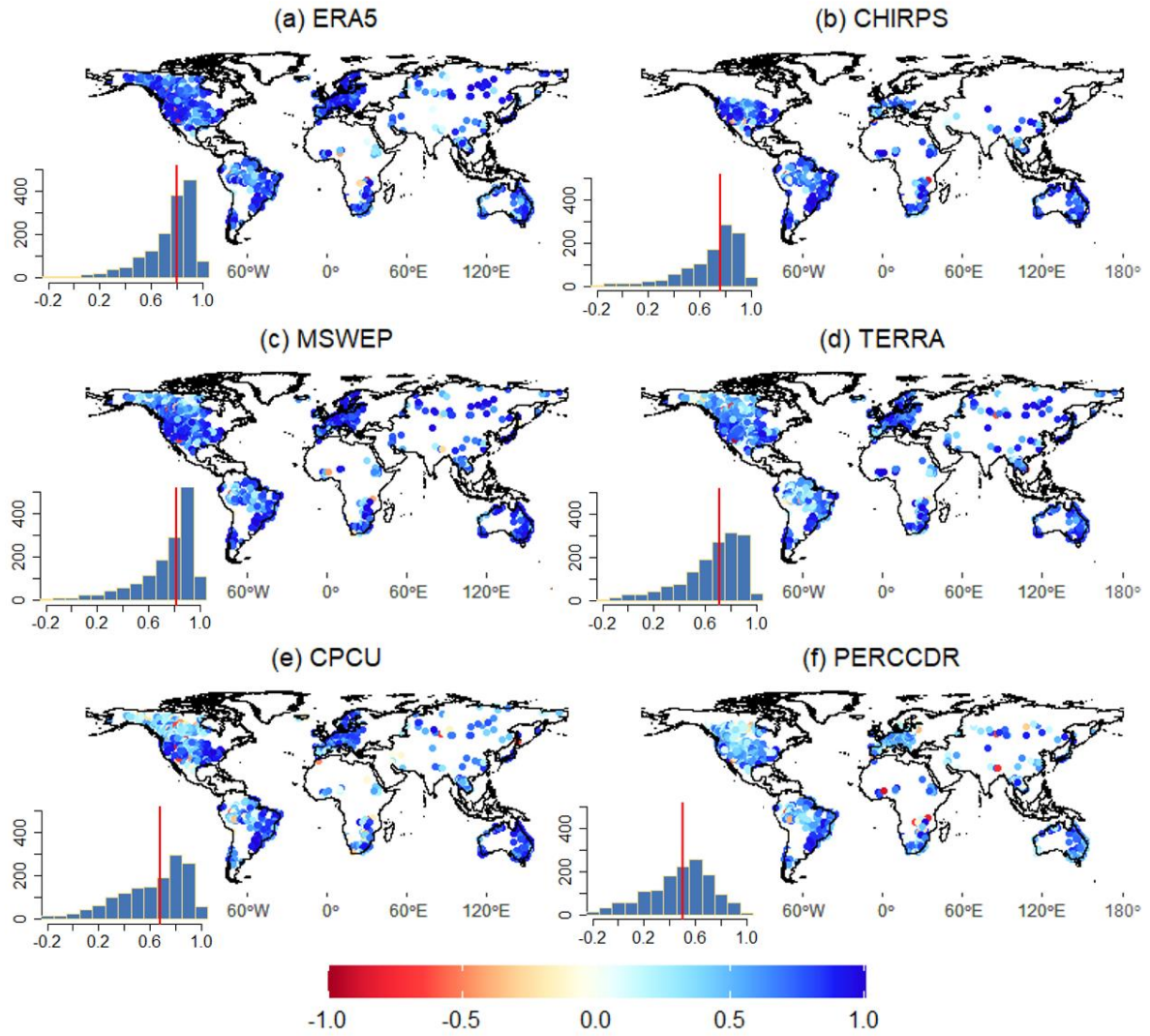
268 
$$NRMSE = \frac{RMSE}{SD} * 100 \quad (5)$$

269 where r is the linear correlation between observed (O) and modelled (M) discharge and  $\alpha$  and  $\beta$  are the variability  
 270 and bias ratios, respectively. The NRMSE and SD are the normalised RMSE and standard deviation, respectively.  
 271 To assess the performance of the precipitation datasets for representing daily hydrological extremes, the 90<sup>th</sup> and  
 272 10<sup>th</sup> percentile are used, which indicates high and low flows, respectively. To derive high and low flow thresholds  
 273 from a daily flow time series, the data is first arranged in ascending order. The 90<sup>th</sup> percentile (Q10) is then  
 274 determined as the flow value above which 90% of the daily flows lie, representing high-flow conditions. Similarly,  
 275 the 10<sup>th</sup> percentile (Q90) represents the flow value below which 90% of the daily flows occur, indicating low-flow  
 276 conditions.

277 **3. Results**

278 **3.1. Performance of the six precipitation datasets for annual discharge prediction**

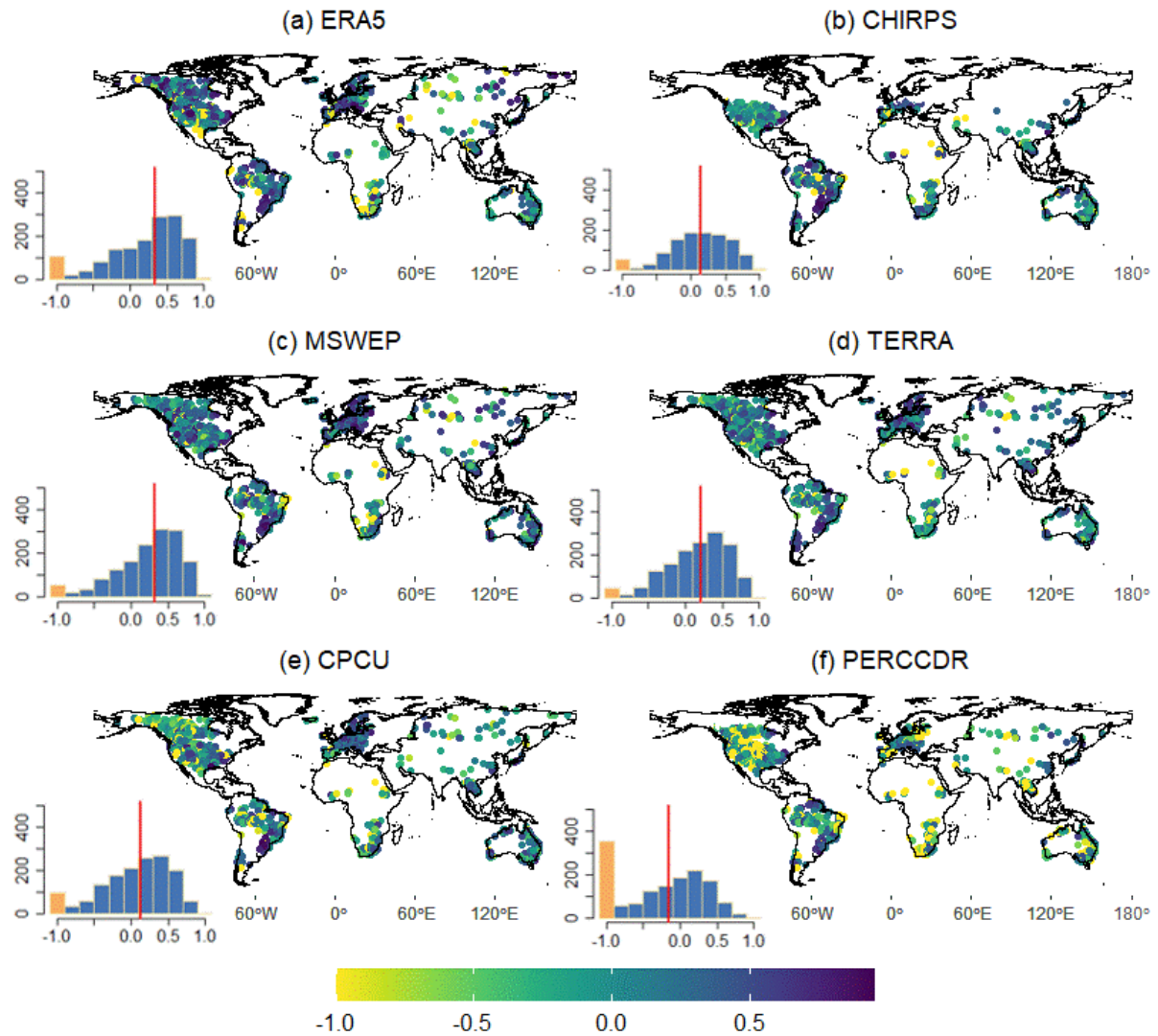
279 The temporal correlation coefficient (CC) between the observed and simulated annual discharge based on the six  
280 precipitation datasets is summarised in Figure 1. Most of the datasets, particularly ERA5, MSWEP, and CHIRPS,  
281 showed a high CC in basins of Europe (e.g., Danube basin), South America (e.g., Rio de la Plata-Parana), North  
282 America and Australia (e.g., Murray-Darling). MSWEP and ERA5 showed the highest CC for 34% and 32% of  
283 the stations, respectively, followed by CPCU and CHIRPS. The TERRA and PERCCDR were the least well-  
284 performing datasets with lower CC overall, and a higher CC than other datasets for less than 9% of stations. The  
285 median CC of MSWEP and ERA5 is 0.82 and 0.8, respectively. MSWEP and TERRA showed lower Pbias and  
286 NRMSE compared to the other datasets (Figures S1 and S2). ERA5 and PERCCDR showed a high NRMSE (up  
287 to 247%) and Pbias (up to 99%) for more than 46% of stations. Similar to the CC, ERA5 and MSWEP  
288 outperformed the other datasets for KGE, with higher values for 32% and 27% of stations, respectively. The  
289 performance of MSWEP and ERA5 is higher in basins of Europe, South America, and Australia compared to Asia  
290 and Africa. The median KGE values of ERA5 and MSWEP are 0.33 and 0.32, respectively (Figure 2). The  
291 PERCCDR and CPU demonstrate high KGE only in about 9% of the stations, with median values of 0.10 and  
292 0.13, respectively. Based on the annual CC and KGE, there is no single precipitation dataset that is best  
293 everywhere, and even the least well-performing dataset overall shows better performance in some stations (Figure  
294 3). Figure 3 summarizes the spatial representation of precipitation dataset performance, highlighting the individual  
295 datasets exhibiting the highest CC and KGE values at each observation point.



296

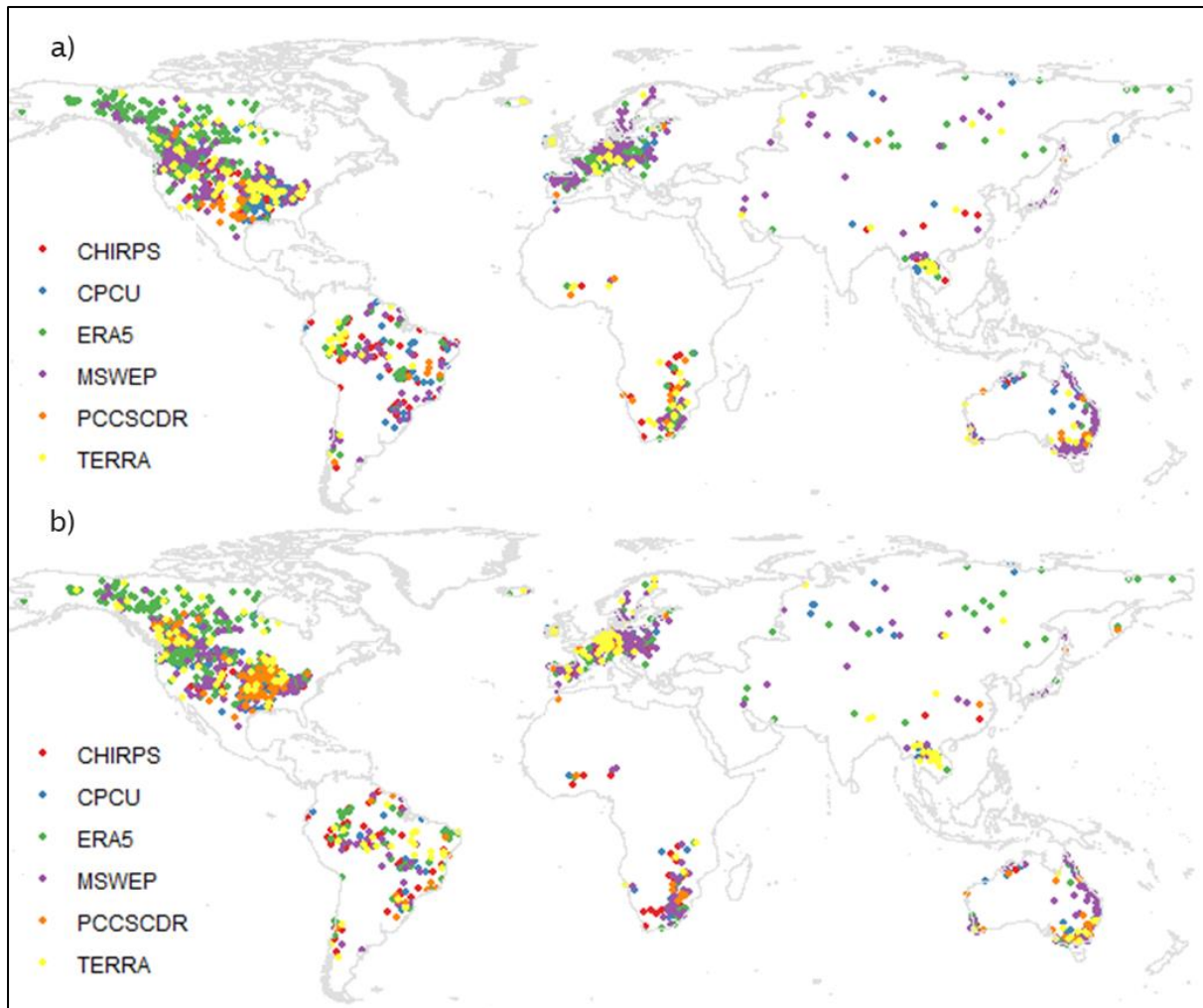
297 **Figure 1: Correlation (CC) between annual observed and modelled streamflow data using a) ERA5, b) CHIRPS, c)**  
 298 **MSWEP, d) TERRA, e) CPCU and f) PERCCDR precipitation datasets. The inset histograms show the frequency**  
 299 **distribution (y-axis) of the annual CC (x-axis), with the red vertical line indicating the median value.**

300



301

302 **Figure 2: KGE between observed and modelled annual streamflow based on a) ERA5, b) CHIRPS, c) MSWEP, d)**  
 303 **TERRA, e) CPCU, and f) PERCCDR precipitation datasets. KGE values below -0.41 indicate bad model performance**  
 304 **than using observed discharge mean as a predictor. The inset histograms show the frequency distribution (y-axis) of**  
 305 **the annual KGE (x-axis). KGE values lower than -1 are highlighted in orange. The red vertical line indicates the median**  
 306 **value.**



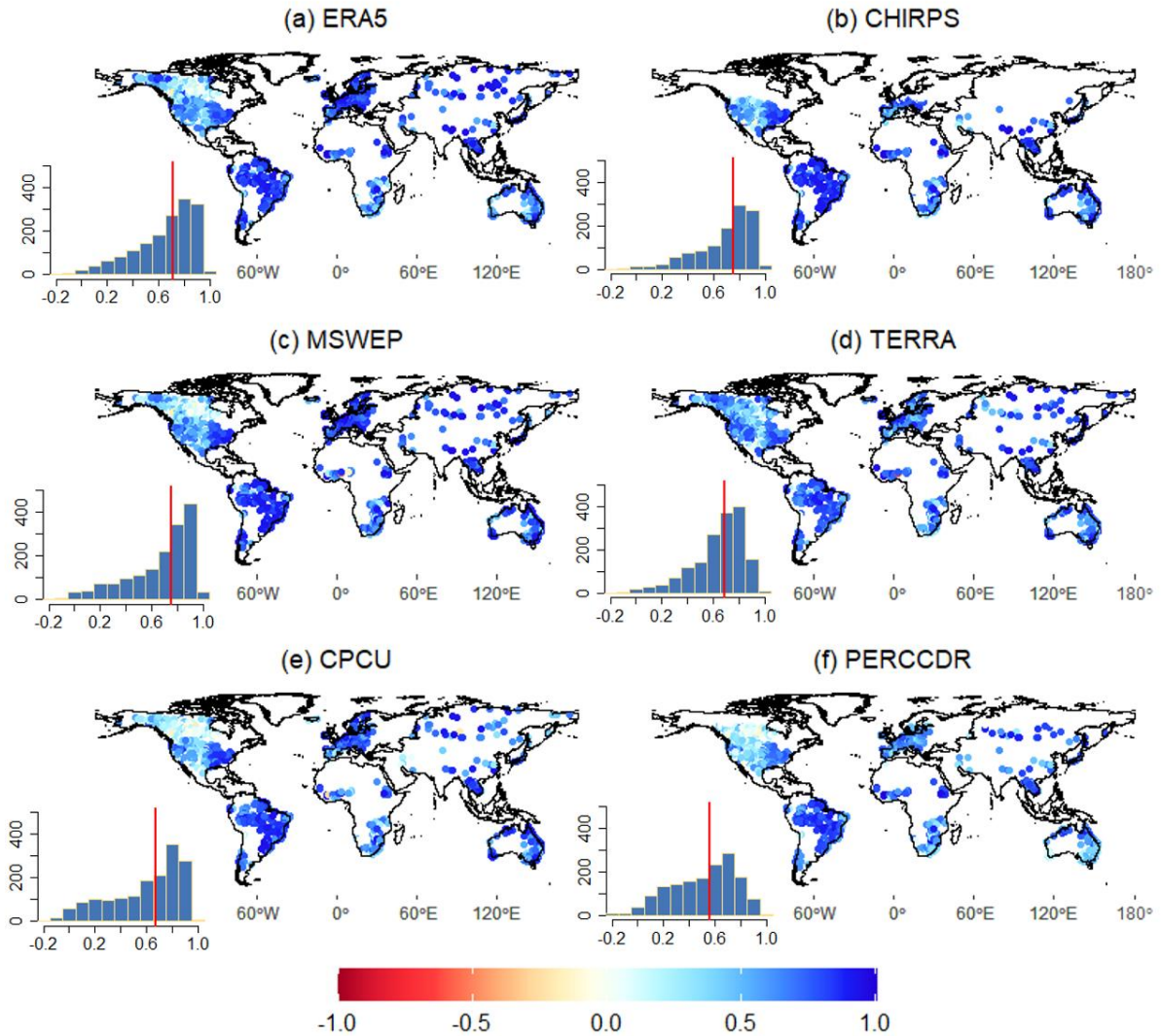
307

308 **Figure 3: The best performing precipitation dataset (ERA5, CHIRPS, MSWEP, TERRA, CPCU, and PERCCDR) at**  
 309 **each of the observed discharge stations based on annual CC (a) and KGE (b).**

310 **3.2. Performance of the six precipitation datasets for monthly discharge predictions**

311 The six precipitation datasets consistently demonstrate high CC at a monthly scale in large parts of the world,  
 312 except in some rivers of Canada and Australia (Figure 4). The monthly CC, similar to the annual CC, shows a  
 313 relatively better performance of MSWEP with a median CC of 0.76. TERRA is the second-best with a median  
 314 CC of 0.69. MSWEP and TERRA show a higher CC than other datasets in 35% and 28% of the stations,  
 315 respectively. ERA5 and CHIRPS are ranked as the third and fourth datasets with a median CC of 0.71 and 0.75,  
 316 respectively. CPCU and PERCCDR are the least well-performing datasets, which only show the highest CC in  
 317 less than 6% of the stations with a median CC of 0.67 and 0.56, respectively.

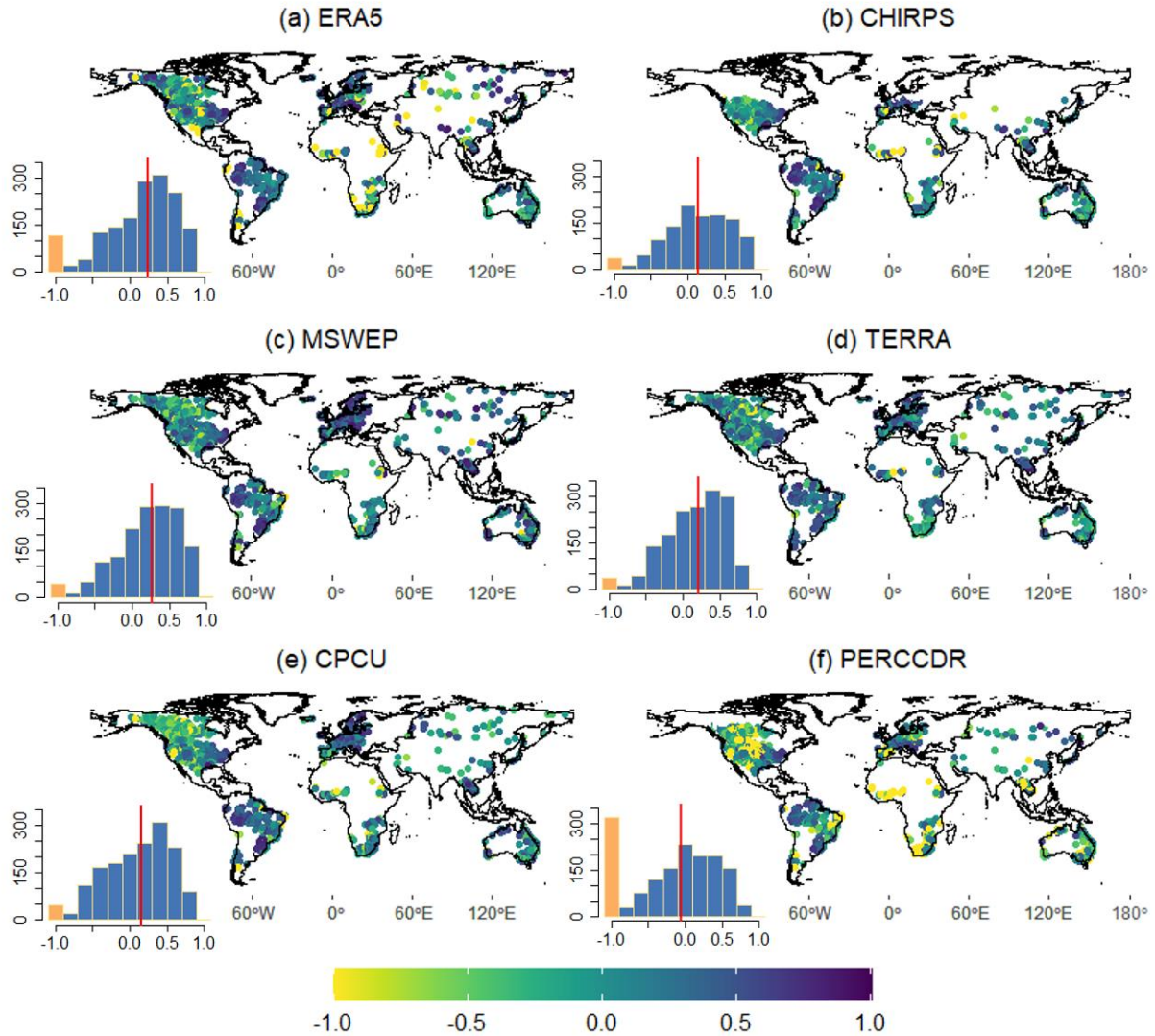




318

319 **Figure 4: Correlation (CC) between monthly observed and modelled streamflow data based on a) ERA5, b) CHIRPS,**  
 320 **c) MSWEP, d) TERRA, e) CPCU and f) PERCCDR precipitation datasets. The inset histograms show the frequency**  
 321 **distribution (y-axis) of the monthly CC (x-axis), with the red vertical line indicating the median value.**

322 The monthly KGE also indicates the better performance of ERA5 and MSWEP for 26% and 24% of stations,  
 323 respectively (Figure 5). MSWEP showed a lower Pbias and NRMSE than all datasets, except in 5% of the stations  
 324 (Figures S3 and S4). Compared to MSWEP, ERA5 showed a larger Pbias and NRMSE in 15% and 19% of the  
 325 stations. TERRA, a third-best performing dataset based on KGE (18% of stations), shows a lower monthly Pbias  
 326 and RMSE in 85% of the stations compared to CHIRPS, ERA5, and PERCCDR. Compared to all datasets, the  
 327 PERCCDR showed a higher NRMSE and Pbias in 55% and 28% of the stations, respectively.

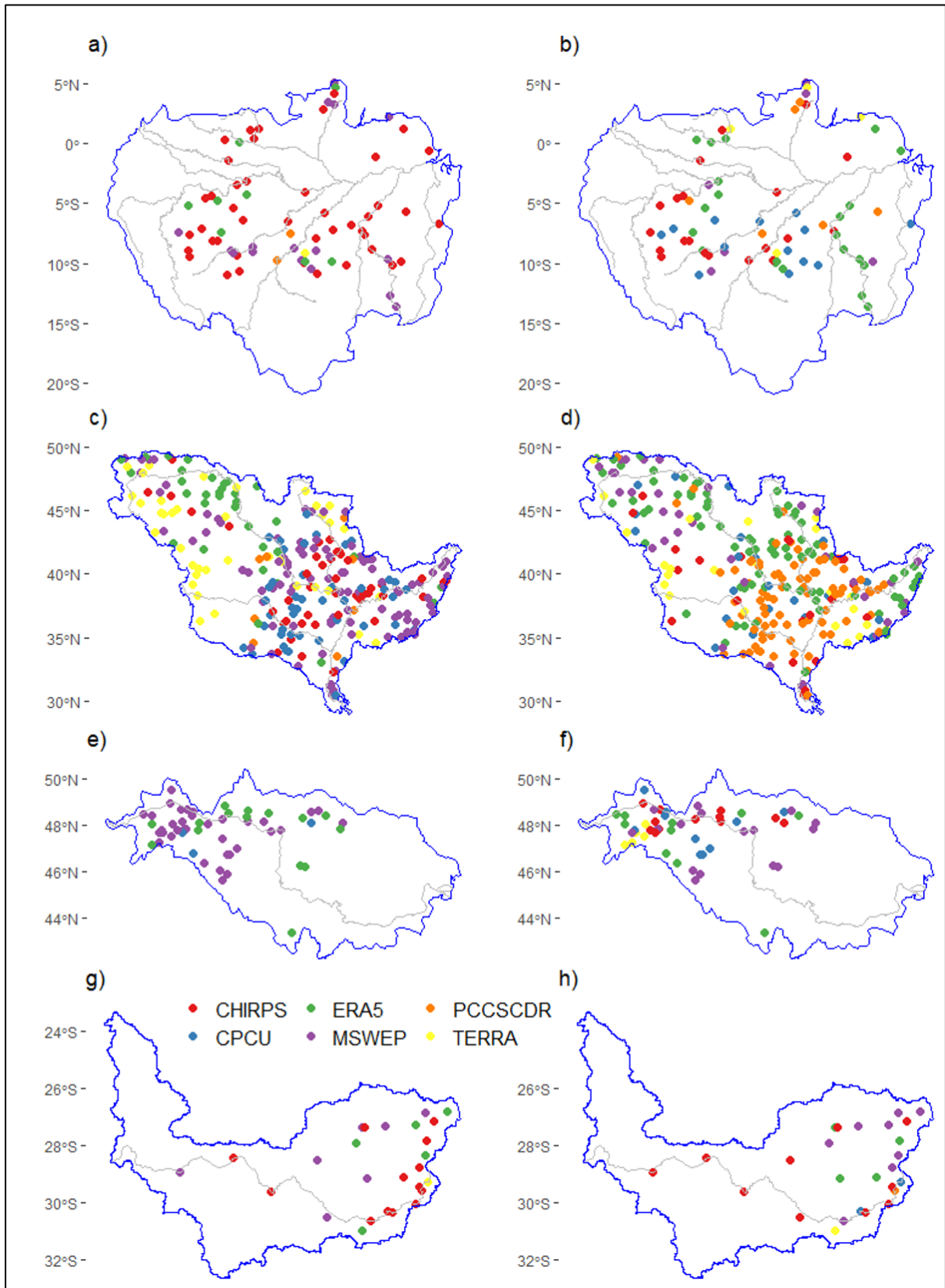


328

329 **Figure 5: Monthly KGE values between observed and modelled streamflow based on a) ERA5, b) CHIRPS, c) MSWEP,**  
 330 **d) TERRA, e) CPCU and f) PERCCDR precipitation datasets. KGE values below -0.41 indicate model performance**  
 331 **that is worse than using the observed discharge mean as a predictor. The inset histograms show the frequency**  
 332 **distribution (y-axis) of the monthly KGE (x-axis). KGE values lower than -1 are highlighted in orange, with the red**  
 333 **vertical line indicating the median value.**

334 The spatial representation of the six precipitation datasets in the Amazon, Mississippi, Danube, and Orange River  
 335 basins is summarised in Figure 6, highlighting the individual datasets exhibiting the highest CC and KGE values  
 336 at each hydrological station. In the Amazon basin, ERA5 (31%) and CHIRPS (29%) emerge as the top performers,  
 337 while PERCCDR (8%) and TERRA (5%) rank lower among the precipitation datasets. In the Mississippi basin,  
 338 MSWEP leads with higher CC in 37% of stations, and ERA5 holds the top products with higher KGE in 31% of  
 339 the stations. Notably, PCCSCDR displays higher KGE values than MSWEP, TERRA, CHIRPS, and CPCU in  
 340 30% of Mississippi stations. Across the Danube basin, MSWEP outperforms the other products with a higher CC  
 341 in 66% of stations and KGE in 30% of the stations, while TERRA and CPCU are the least performing products.  
 342 Furthermore, CHIRPS, in 52% of stations based on CC and 37% based on KGE, outperformed other datasets in

343 the Orange River basin. In Orange, MSWEP ranks second with higher KGE and CC in about 27% of stations,  
344 while TERRA and PCCSCDR are the least performing datasets.



345



346 **Figure 6: Performance of precipitation datasets (ERA5, CHIRPS, MSWEP, TERRA, CPCU, and PERCCDR) at**  
 347 **discharge stations in a) Amazon, c) Mississippi, e) Danube, and g) Orange river basins based on their monthly CC.**  
 348 **Performance of the datasets based on KGE for the Amazon, Mississippi, Danube, and Orange River Basins is illustrated**  
 349 **in figures b, d, f, and h, respectively.**

350 Table 2 summarises the monthly KGE between observed and modelled streamflow, based on the six precipitation  
 351 datasets, for selected locations in basins of Africa (Niger, Lokoja), Asia (Mekong, Khong-Chiam), South America  
 352 (Amazon, Missao-Icana), North America (Mississippi, Savannah), Australia (North East Coast, Mirani-Weir),  
 353 and Europe (Danube, Dunaalmas). The basins were chosen to represent a good range of climatic regions and  
 354 drainage areas where there was availability of a long time series of observed data (Figure S5). In Niger, the  
 355 observed monthly flow and variability at Lokoja station are very well reproduced by CHIRPS and TERRA with  
 356 a CC of 0.88 and 0.85, respectively (Figure S5a). Even though CPCU showed a lower CC (0.64) at Lokoja, it  
 357 showed a higher KGE (0.62) and lower Pbias (0.4%) compared to the other products. At Lokoja, PERCCDR is  
 358 the least well-performing dataset with the highest RMSE and Pbias and lowest KGE. The monthly variability at  
 359 the Khong-Chiam station is reproduced by all the precipitation products with a CC of greater than 0.91, with  
 360 MSWEP and TERRA showing the lowest bias and RMSE. ERA5 and CHIRPS performed well at station Missao-  
 361 Icana in the Amazon with a CC of 0.9 and RMSE of about 610 m3/s. For stations Savannah, Mirani-Weir, and  
 362 Dunaalmas, MSWEP is the best product with higher CC (> 0.72) and KGE (> 0.62) and lower Pbias and RMSE  
 363 (Figure S5d - S5f).

364 Table 2. KGE of monthly predictions for selected stations in basins of Africa (Niger), Asia (Mekong), South  
 365 America (Amazon), North America (Mississippi), Australia (North East Coast), and Europe (Danube).

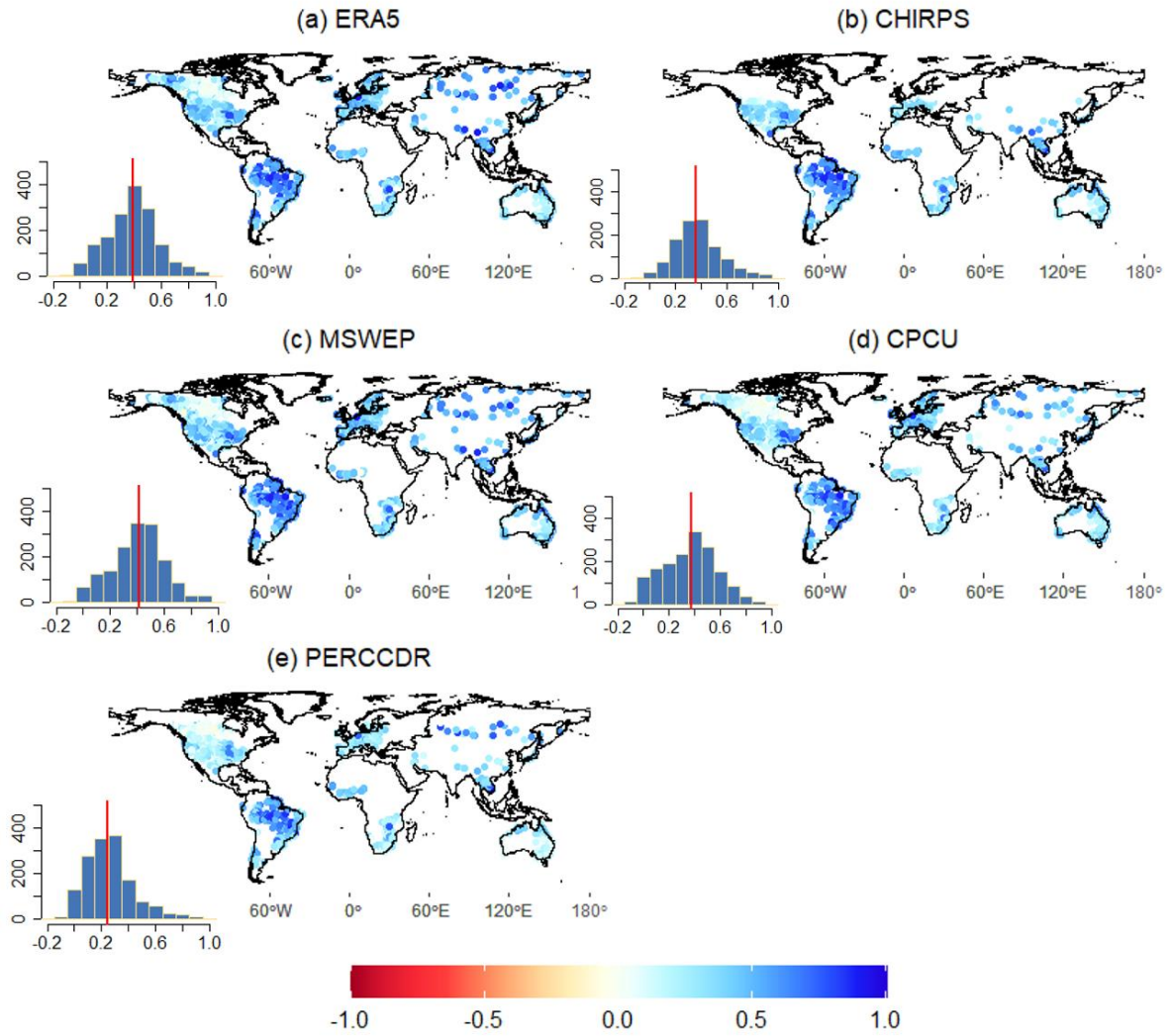
Basin	Stations name	Longitude	Latitude	Catchment area (km <sup>2</sup> )	ERA5	CHIRPS	MSWEP	TERRA	CPCU	PERCCDR
Niger	Lokoja	6.8	7.8	1670000	0.21	-0.1	0.60	0.34	0.62	-0.99
Mekong	Khong Chiam	105.5	15.3	419000	0.13	0.56	0.70	0.91	0.70	-0.04
Amazon	Missao Icana	-67.6	1.1	22282	0.71	0.78	0.73	0.72	0.61	0.65
Mississippi	Savannah	-88.3	35.2	85833	0.59	0.65	0.67	0.66	0.53	0.66
North East Coast	Mirani-Weir	148.8	-21.2	1211	-0.1	0.38	0.62	0.44	0.46	-0.05
Danube	Dunaalmas	18.3	47.7	171720	0.34	0.73	0.78	0.52	0.71	-0.49

366

367

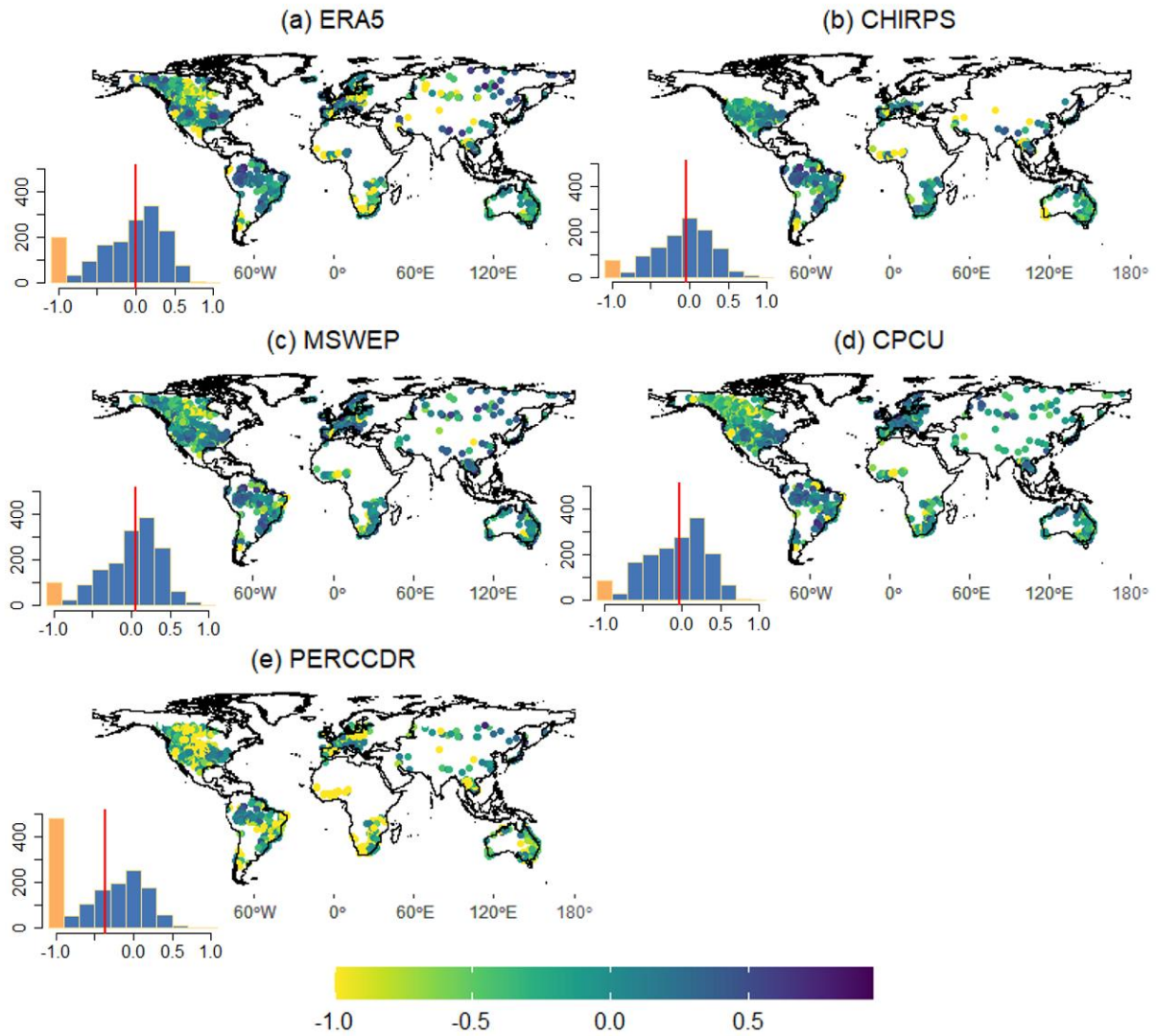
368 **3.3. Performance of the precipitation datasets for daily and daily extreme discharge predictions**

369 Based on the daily evaluation, MSWEP followed by ERA5 show a higher CC in more than 50% of the stations  
370 with median values of 0.41 and 0.39, respectively (Figure 7). ERA5 and MSWEP performed well in 31% and  
371 31% of the stations with high KGE values (Figure 8). Similar to the monthly evaluation, PERCCDR shows poorer  
372 performance (lower CC and KGE, higher biases and errors) in almost 95% of the stations. Even though ERA5  
373 showed a higher CC and KGE in 30% of the stations it shows a higher NRMSE (up to 250%) and Pbias (up to  
374 100%) in 20% and 30% of the stations (Figures S6 and S7). Overall, MSWEP and CHIRPS showed lower NRMSE  
375 and Pbias compared to the other products. The CC and KGE of all the products (except CHIRPS) are lower in  
376 North America compared to stations in South America, Europe, and Australia. The spatial representation of  
377 precipitation dataset performance, highlighting the individual datasets exhibiting the highest daily CC and KGE  
378 values at each observation point, is provided in Figure S9. Additionally, Figure S10 depicts the spatial  
379 representation of each precipitation dataset for the Amazon, Mississippi, Danube, and Orange River Basins. In  
380 Mississippi, ERA5 exhibited the highest KGE and CC values, followed by MSWEP and CPCU (Figure S10). In  
381 the Amazon, ERA5 and CHIRPS displayed the highest KGE and CC values compared to the other datasets. For  
382 the Danube, CPCU followed by MSWEP emerged as the best precipitation product relative to ERA5, PCCSCDR,  
383 and CHIRPS. In the Orange River Basin, MSWEP based on CC and CHIRPS based on KGE were the top-  
384 performing products, while PCCSCDR performed the least.



385

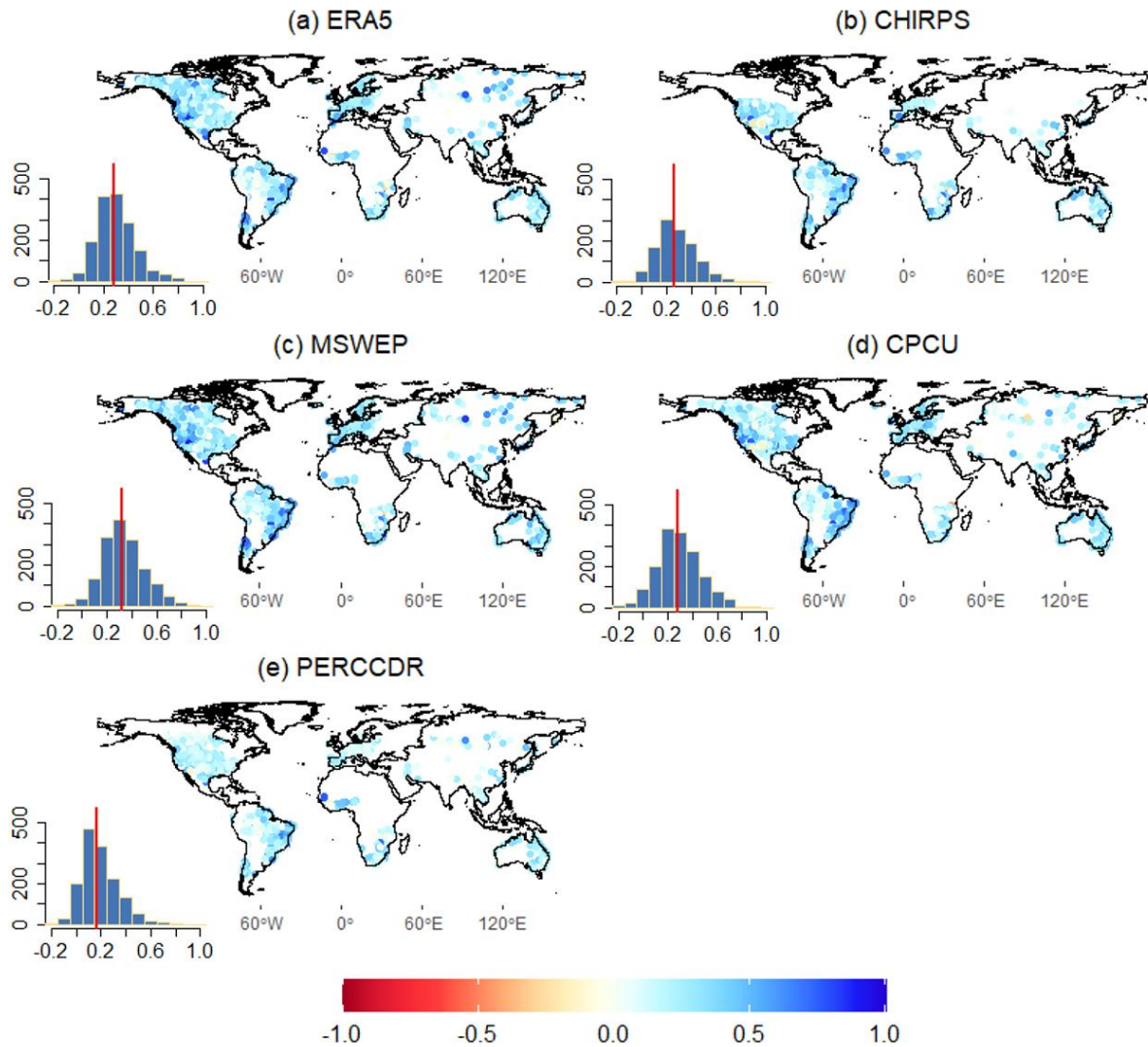
386 Figure 7: Correlation (CC) between daily observed and modelled streamflow data using a) ERA5, b) CHIRPS, c)  
 387 MSWEP, d) CPCU and e) PERCCDR precipitation datasets. The inset histograms show the frequency distribution (y-  
 388 axis) of the daily CC (x-axis), with the red vertical line indicating the median value.



389

390 **Figure 8: Daily KGE values between observed and modelled streamflow based on a) ERA5, b) CHIRPS, c) MSWEP,**  
 391 **d) CPCU, and e) PERCCDR precipitation datasets. KGE values below -0.41 indicate bad model performance than**  
 392 **using observed discharge mean as a predictor. The inset histograms show the frequency distribution (y-axis) of the**  
 393 **daily KGE (y-axis). KGE values lower than -1 are highlighted in orange, with the red vertical line indicating the median**  
 394 **value.**

395 The performance of the daily precipitation products is also assessed for daily extremes in terms of the Q10 and  
 396 Q90 values. Based on the CC, MSWEP is the best-performing dataset for Q10 (Figure 9) and Q90 (Figure S8).  
 397 For Q10, MSWEP and CPCU exhibited a higher CC than other datasets at 38% and 32% of the stations,  
 398 respectively. Similarly, for Q90, MSWEP and ERA demonstrated a higher CC compared to other datasets at 35%  
 399 and 30% of the stations. The median CC for Q10 (Q90) is 0.32 (0.41), 0.28 (0.36), 0.27 (0.35), 0.26 (0.38), and  
 400 0.16 (0.23) for MSWEP, CPCU, CHIRPS, ERA5, CHIRPS, and PERCCDR, respectively. Similar to the annual,  
 401 monthly and daily evaluations, PERCCDR showed poor performance for the two extremes (Q90 and Q10).  
 402 Overall, the performance of the datasets is lower for extremes compared to the annual, monthly and daily scales.



403

404 **Figure 9: Correlation (CC) between observed and modelled daily extremes (Q10, high flow) streamflow data a) ERA5,**  
 405 **b) CHIRPS, c) MSWEP, d) CPCU and e) PERCCDR precipitation datasets. The inset histograms show the frequency**  
 406 **distribution (y-axis) of the daily Q10 CC (x-axis), with the red vertical line indicating the median value.**

407 **4. Discussion and Conclusion**

408 Based on the evaluation at annual, monthly and daily time scales and analysis of daily extremes, no single  
 409 precipitation dataset consistently exhibits high accuracy across all geographical regions, nor is one consistently  
 410 better than the other datasets. This finding is in line with previous studies (Beck et al., 2017a; Dembélé et al.,  
 411 2020). A similar pattern of varied performance (e.g., lower in Africa and the central United States and better in  
 412 Europe) by different global hydrological models and precipitation datasets has been presented (Beck et al., 2017a;  
 413 Lin et al., 2019; Harrigan et al., 2020). In addition to the uncertainty in the precipitation datasets, the poorer  
 414 performance in some regions presented in this and previous studies (Beck et al., 2017a; Lin et al., 2019; Harrigan  
 415 et al., 2020) can be due to the lack of representation in the hydrological models of anthropogenic influences, such  
 416 as for agriculture, irrigation, water supply, and energy production.

417 Comparably, MSWEP and ERA5 consistently exhibited higher CC and KGE values at over 50% of the stations  
418 across annual, monthly, and daily time scales. According to Gu et al. (2023), satellite- and reanalysis-based  
419 precipitation datasets, such as MSWEP and ERA5, can provide satisfactory performance for simulating discharge  
420 globally. The higher performance of MSWEP indicates the advantage of incorporating a large number of daily  
421 observations from field-based meteorological stations, in addition to a large set of satellite and reanalysis datasets  
422 (Beck et al., 2017a, 2019a). Other studies have also shown the good performance of MSWEP for hydrological  
423 modelling in different parts of the world (Beck et al., 2017a; Lakew, 2020; Li et al., 2022a; Reis et al., 2022; Gu  
424 et al., 2023; López López et al., 2017; Satgé et al., 2019; Ibrahim et al., 2022). For example, Satgé et al. (2019)  
425 evaluated 12 satellite-based precipitation estimates such as MSWEP, CHIRPS and PERSIANN-CDR in South  
426 America (Lake Titicaca region) and found MSWEP was the best precipitation dataset for realistic simulation of  
427 river discharge. MSWEP was also found to be the most reliable precipitation dataset compared to multiple datasets  
428 such as CHIRPS and CMORPH for hydrological and climate studies in basins of Eastern China (Shaowei et al.,  
429 2022; Wu et al., 2018).

430 Even though ERA5 showed a higher KGE and CC than MSWEP, CHIRPS and TERRA in about 32% of the  
431 stations it showed a higher error and biases. Previous studies have revealed bias and errors in ERA5 precipitation  
432 (Lavers et al., 2021; Bechtold et al., 2020; AL-Falahi et al., 2020; Jiang et al., 2023; Lavers et al., 2022), which  
433 leads to propagated errors and bias in hydrological modelling outputs. Harrigan et al. (2020) also reported large  
434 biases in ERA5-driven hydrological simulations in the Central United States, South America (e.g., Brazil), and  
435 Africa. According to Lavers et al. (2022), ERA5 precipitation is more reliable in extratropical areas compared to  
436 tropical areas. Despite CPCU being a gauge-based precipitation dataset, it did not show as good performance as  
437 MSWEP and ERA5 on annual, monthly, and daily timescales. In addition to the lower KGE and CC, CPCU  
438 showed higher bias and error, particularly on annual and monthly time scales. The bias and errors in CPCU can  
439 be due to the coarse resolution (0.5°) and the limited number of stations used to develop the datasets, particularly  
440 in Africa and South America. According to Beck et al. (2017a), CPCU can be used in large river basins with dense  
441 meteorological stations but can be disadvantageous in Africa and South America. This highlights the need to  
442 expand and maintain the meteorological stations in these regions, but also the need to draw from satellite and  
443 model data sources. The PERSIANN-CDR is the least-performing product with lower KGE and higher errors and  
444 biases, which has been highlighted elsewhere in terms of its inability to represent precipitation extremes (Miao et  
445 al., 2015; Solakian et al., 2020).

446 The precipitation datasets show limited skill overall in reproducing daily extremes (high and low flows), relative  
447 to the annual and monthly time scales. MSWEP and CPCU have shown a high CC in about 38% of the stations.  
448 This is consistent with the findings of Tang et al., (2019) for the Mekong River Basin. CHIRPS and PERSIANN-  
449 CDR are the least skilful in capturing extremes with a very low CC and large positive and negative biases (Araujo  
450 Palharini et al., 2021). For instance, numerous precipitation products have been observed to both underestimate  
451 and overestimate low and high precipitation values in Brazil (Palharini et al., 2020), consequently resulting in  
452 corresponding underestimations and overestimations of low and high streamflows. In general, several studies have  
453 concluded that precipitation datasets exhibit a substantial disparity in daily extreme precipitation events (e.g.,  
454 Araujo Palharini et al., 2021; Jiang et al., 2019; Huang et al., 2022), which can be attributed to factors such as  
455 inaccuracies in satellite sensors, retrieval algorithms, temporal sampling, and satellite-observation merging and

456 bias correction procedures used, particularly in gauge-limited regions (Miao et al., 2015; El Kenawy et al., 2015;  
457 Shen et al., 2010; Jiang et al., 2019). In addition to the uncertainty of the precipitation datasets, the limited  
458 availability of hydrological observations limits the ability to assess these datasets globally, especially for extreme  
459 flood and drought events (Brunner et al., 2021).

460 While our study evaluates six global precipitation datasets for hydrological modelling using WBMsed, which  
461 show an  $R^2$  of 0.99 in 30-year average prediction against USGS gauge data and global river datasets (Cohen et  
462 al., 2022), it is important to acknowledge uncertainties and limitations in both the precipitation data and model  
463 parameters. Uncertainties in input data, such as those derived from satellite-based precipitation datasets, including  
464 retrieval errors, can propagate through the hydrological model, potentially affecting the accuracy of simulated  
465 discharge. Additionally, globally calibrated model parameters may introduce further uncertainty, particularly in  
466 regions with limited observational data coverage. Due to the limited availability of observed discharge in Africa  
467 and Asia, the evaluation predominantly focuses on North and South America and Europe. Hence, further  
468 evaluation in Africa and Asia could be essential to enhance the robustness of global hydrological models.

469 Overall, the evaluation presented in this paper underlines the importance of selecting high-quality precipitation  
470 datasets to drive hydrological models. Since no single precipitation dataset was found to be adequately accurate  
471 everywhere, this study can help identify the best precipitation products for any basin or region under consideration.  
472 Based on our results, MSWEP is the best overall choice but there are regions where ERA5, CHIRPS and CPCU  
473 were better overall. All the precipitation datasets, particularly ERA5 and PERCCDR, require bias correction  
474 before being used to drive hydrological models in regions like North America, Asia, Africa, and Australia. For  
475 data-scarce regions such as Africa and Asia, it is difficult to recommend a precipitation dataset due to the limited  
476 number of hydrological stations used in this study. Finally, improving the precipitation datasets by adding more  
477 ground observations, for example, and by better representing anthropogenic drivers in hydrological models has  
478 the potential of considerably improving global and regional hydrological predictions.

#### 479 **Data availability**

480 The selected precipitation datasets used in this study are openly accessible to the public. ERA5 is freely available  
481 from the Copernicus Climate Data Store (CDS; <https://cds.climate.copernicus.eu/cdsapp#!/dataset/reanalysis-era5-land?tab=overview>). CHIRPS can be obtained from the Climate Hazards Group (CHG; <https://www.chc.ucsb.edu/data/chirps/>). Access to the MSWEP precipitation dataset is provided through the  
483 GloH2O website (<https://www.gloh2o.org/mswep/>). TERRA is accessible from the Climatology Lab website  
484 (<https://www.climatologylab.org/>). CPCU is publicly available through the NOAA Physical Sciences Laboratory  
485 (PSL; [https://downloads.psl.noaa.gov/Datasets/cpc\\_global\\_precip/](https://downloads.psl.noaa.gov/Datasets/cpc_global_precip/)), and PERCCDR can be freely accessed  
486 through the Center for Hydrometeorology and Remote Sensing (CHRS; <https://chrsdata.eng.uci.edu/>).

#### 488 **Author contribution**



489 SG, JL, and SJD: conceptualization. SG: methodology and formal analysis, writing – original draft preparation.  
490 JL, SJD, and LS: resources. SC: software and data curation. MW, GB, and RB: investigation, writing – review &  
491 editing. PD, HG, and EV: data curation and visualization. YL, RH, LH, SM, and JN: methodology, visualization,  
492 investigation, writing – review & editing. PA, HC, AN, AT, and JS: formal analysis, resources, writing – review  
493 & editing. DP, SJD, and SED: supervision and project administration.

494 ~~SG, JL, and SJD conceived the study, incorporating input from all co-authors. SG led the global hydrological~~  
495 ~~modelling, while JL, SJD, and LS assisted with data management and computational resources. SG was~~  
496 ~~responsible for evaluating various precipitation datasets for hydrological modelling and drafted the initial~~  
497 ~~manuscript. SC provided the hydrological model and input parameters. MW, GB, RB, PD, HG, EV, YL, RH, LH,~~  
498 ~~SM, and JN executed extensive data quality control and identified stations for evaluation. PA, HC, AN, AT, and~~  
499 ~~JS provided code, methods, and guidance. DP, SJD, and SED supervised the research and secured funding. All~~  
500 ~~authors contributed to investigating research findings and played integral roles in manuscript writing and editing.~~

### 501 **Competing interests**

502 We declare that Louise Slater is a topical editor of Hydrology and Earth System Sciences (HESS).

### 503 **Acknowledgements**

504 This work is part of the Evolution of Global Flood Hazard and Risk (EVOFLOOD) project [NE/S015817/1]  
505 supported by the Natural Environment Research Council (NERC), the UK Foreign, Commonwealth and  
506 Development Office (FCDO) for the benefit of developing countries (Programme Code 201880) and the UK's  
507 Natural Environment Research Council (NERC; NE/S017380/1).

508

509

510

511

512

513

514

515

516

517



518

519

520 Reference

- 521 Abatzoglou, J. T., Dobrowski, S. Z., Parks, S. A., and Hegewisch, K. C.: TerraClimate, a high-resolution global  
522 dataset of monthly climate and climatic water balance from 1958–2015, *Sci Data*, 5, 170191,  
523 <https://doi.org/10.1038/sdata.2017.191>, 2018.
- 524 Acharya, S. C., Nathan, R., Wang, Q. J., Su, C.-H., and Eizenberg, N.: An evaluation of daily precipitation from  
525 a regional atmospheric reanalysis over Australia, *Hydrology and Earth System Sciences*, 23, 3387–3403,  
526 <https://doi.org/10.5194/hess-23-3387-2019>, 2019.
- 527 Ahmed, K., Shahid, S., Wang, X., Nawaz, N., and Khan, N.: Evaluation of Gridded Precipitation Datasets over  
528 Arid Regions of Pakistan, *Water*, 11, 210, <https://doi.org/10.3390/w11020210>, 2019.
- 529 Alazzy, A. A., Lü, H., Chen, R., Ali, A. B., Zhu, Y., and Su, J.: Evaluation of Satellite Precipitation Products  
530 and Their Potential Influence on Hydrological Modeling over the Ganzi River Basin of the Tibetan Plateau,  
531 *Advances in Meteorology*, 2017, e3695285, <https://doi.org/10.1155/2017/3695285>, 2017.
- 532 AL-Falahi, A. H., Saddique, N., Spank, U., Gebrechorkos, S. H., and Bernhofer, C.: Evaluation the Performance  
533 of Several Gridded Precipitation Products over the Highland Region of Yemen for Water Resources  
534 Management, *Remote Sensing*, 12, 2984, <https://doi.org/10.3390/rs12182984>, 2020.
- 535 Araujo Palharini, R. S., Vila, D. A., Rodrigues, D. T., Palharini, R. C., Mattos, E. V., and Pedra, G. U.:  
536 Assessment of extreme rainfall estimates from satellite-based: Regional analysis, *Remote Sensing Applications:  
537 Society and Environment*, 23, 100603, <https://doi.org/10.1016/j.rsase.2021.100603>, 2021.
- 538 Bárdossy, A., Kilsby, C., Birkinshaw, S., Wang, N., and Anwar, F.: Is Precipitation Responsible for the Most  
539 Hydrological Model Uncertainty?, *Frontiers in Water*, 4, 2022.
- 540 Bechtold, P., R Forbes, I Sandu, S Lang, and M Ahlgrimm: A major moist physics upgrade for the IFS, , 24–32,  
541 2020.
- 542 Beck, H. E., Vergopolan, N., Pan, M., Levizzani, V., Dijk, A. I. J. M. van, Weedon, G. P., Brocca, L.,  
543 Pappenberger, F., Huffman, G. J., and Wood, E. F.: Global-scale evaluation of 22 precipitation datasets using  
544 gauge observations and hydrological modeling, *Hydrology and Earth System Sciences*, 21, 6201–6217,  
545 <https://doi.org/10.5194/hess-21-6201-2017>, 2017a.
- 546 Beck, H. E., van Dijk, A. I. J. M., Levizzani, V., Schellekens, J., Miralles, D. G., Martens, B., and de Roo, A.:  
547 MSWEP: 3-hourly 0.25° global gridded precipitation (1979–2015) by merging gauge, satellite, and reanalysis  
548 data, *Hydrology and Earth System Sciences*, 21, 589–615, <https://doi.org/10.5194/hess-21-589-2017>, 2017b.
- 549 Beck, H. E., Pan, M., Roy, T., Weedon, G. P., Pappenberger, F., van Dijk, A. I. J. M., Huffman, G. J., Adler, R.  
550 F., and Wood, E. F.: Daily evaluation of 26 precipitation datasets using Stage-IV gauge-radar data for the  
551 CONUS, *Hydrology and Earth System Sciences*, 23, 207–224, <https://doi.org/10.5194/hess-23-207-2019>,  
552 2019a.
- 553 Beck, H. E., Wood, E. F., Pan, M., Fisher, C. K., Miralles, D. G., Dijk, A. I. J. M. van, McVicar, T. R., and  
554 Adler, R. F.: MSWEP V2 Global 3-Hourly 0.1° Precipitation: Methodology and Quantitative Assessment,  
555 *Bulletin of the American Meteorological Society*, 100, 473–500, <https://doi.org/10.1175/BAMS-D-17-0138.1>,  
556 2019b.
- 557 Brunner, M. I., Slater, L., Tallaksen, L. M., and Clark, M.: Challenges in modeling and predicting floods and  
558 droughts: A review, *WIREs Water*, 8, e1520, <https://doi.org/10.1002/wat2.1520>, 2021.
- 559 Chen, M., Shi, W., Xie, P., Silva, V. B. S., Kousky, V. E., Wayne Higgins, R., and Janowiak, J. E.: Assessing  
560 objective techniques for gauge-based analyses of global daily precipitation, *Journal of Geophysical Research:  
561 Atmospheres*, 113, <https://doi.org/10.1029/2007JD009132>, 2008.
- 562 Chen, Y., Hu, D., Duan, X., Zhang, Y., Liu, M., and Shasha, W.: Rainfall-runoff simulation and flood dynamic  
563 monitoring based on CHIRPS and MODIS-ET, *International Journal of Remote Sensing*, 41, 4206–4225,  
564 <https://doi.org/10.1080/01431161.2020.1714779>, 2020.
- 565 Cohen, S., Kettner, A. J., Syvitski, J. P. M., and Fekete, B. M.: WBMsed, a distributed global-scale riverine  
566 sediment flux model: Model description and validation, *Computers & Geosciences*, 53, 80–93,  
567 <https://doi.org/10.1016/j.cageo.2011.08.011>, 2013.
- 568 Cohen, S., Kettner, A. J., and Syvitski, J. P. M.: Global suspended sediment and water discharge dynamics  
569 between 1960 and 2010: Continental trends and intra-basin sensitivity, *Global and Planetary Change*, 115, 44–  
570 58, <https://doi.org/10.1016/j.gloplacha.2014.01.011>, 2014.

571 Cohen, S., Syvitski, J., Ashley, T., Lammers, R., Fekete, B., and Li, H.-Y.: Spatial Trends and Drivers of  
572 Bedload and Suspended Sediment Fluxes in Global Rivers, *Water Resources Research*, 58, e2021WR031583,  
573 <https://doi.org/10.1029/2021WR031583>, 2022.

574 Day, C. A. and Howarth, D. A.: Modeling Climate Change Impacts on the Water Balance of a Medium-Scale  
575 Mixed-Forest Watershed, SE USA, *Southeastern Geographer*, 59, 110–129, 2019.

576 Dembélé, M., Schaeffli, B., van de Giesen, N., and Mariéthoz, G.: Suitability of 17 gridded rainfall and  
577 temperature datasets for large-scale hydrological modelling in West Africa, *Hydrology and Earth System  
578 Sciences*, 24, 5379–5406, <https://doi.org/10.5194/hess-24-5379-2020>, 2020.

579 Dunn, F. E., Darby, S. E., Nicholls, R. J., Cohen, S., Zarfl, C., and Fekete, B. M.: Projections of declining  
580 fluvial sediment delivery to major deltas worldwide in response to climate change and anthropogenic stress,  
581 *Environ. Res. Lett.*, 14, 084034, <https://doi.org/10.1088/1748-9326/ab304e>, 2019.

582 Eini, M. R., Rahmati, A., and Piniewski, M.: Hydrological application and accuracy evaluation of PERSIANN  
583 satellite-based precipitation estimates over a humid continental climate catchment, *Journal of Hydrology:  
584 Regional Studies*, 41, 101109, <https://doi.org/10.1016/j.ejrh.2022.101109>, 2022.

585 El Kenawy, A. M., Lopez-Moreno, J. I., McCabe, M. F., and Vicente-Serrano, S. M.: Evaluation of the TMPA-  
586 3B42 precipitation product using a high-density rain gauge network over complex terrain in northeastern Iberia,  
587 *Global and Planetary Change*, 133, 188–200, <https://doi.org/10.1016/j.gloplacha.2015.08.013>, 2015.

588 Fallah, A., Rakhshandehroo, G. R., Berg, P., O, S., and Orth, R.: Evaluation of precipitation datasets against  
589 local observations in southwestern Iran, *International Journal of Climatology*, 40, 4102–4116,  
590 <https://doi.org/10.1002/joc.6445>, 2020.

591 Funk, C., Peterson, P., Landsfeld, M., Pedreros, D., Verdin, J., Shukla, S., Husak, G., Rowland, J., Harrison, L.,  
592 Hoell, A., and Michaelsen, J.: The climate hazards infrared precipitation with stations—a new environmental  
593 record for monitoring extremes, *Scientific Data*, 2, 150066, <https://doi.org/10.1038/sdata.2015.66>, 2015.

594 Gebrechorkos, S. H., Hülsmann, S., and Bernhofer, C.: Evaluation of multiple climate data sources for  
595 managing environmental resources in East Africa, *Hydrology and Earth System Sciences*, 22, 4547–4564,  
596 <https://doi.org/10.5194/hess-22-4547-2018>, 2018.

597 Gebrechorkos, S. H., Bernhofer, C., and Hülsmann, S.: Impacts of projected change in climate on water balance  
598 in basins of East Africa, *Science of The Total Environment*, <https://doi.org/10.1016/j.scitotenv.2019.05.053>,  
599 2019.

600 Gebrechorkos, S. H., Bernhofer, C., and Hülsmann, S.: Climate change impact assessment on the hydrology of a  
601 large river basin in Ethiopia using a local-scale climate modelling approach, *Science of The Total Environment*,  
602 742, 140504, <https://doi.org/10.1016/j.scitotenv.2020.140504>, 2020.

603 Gebrechorkos, S. H., Leyland, J., Darby, S., and Parsons, D.: High-resolution daily global climate dataset of  
604 BCCAQ statistically downscaled CMIP6 models for the EVOFLOOD project. NERC EDS Centre for  
605 Environmental Data Analysis, <https://doi.org/10.5285/C107618F1DB34801BB88A1E927B82317>, 2022a.

606 Gebrechorkos, S. H., Pan, M., Beck, H. E., and Sheffield, J.: Performance of State-of-the-Art C3S European  
607 Seasonal Climate Forecast Models for Mean and Extreme Precipitation Over Africa, *Water Resources Research*,  
608 58, e2021WR031480, <https://doi.org/10.1029/2021WR031480>, 2022b.

609 Gebrechorkos, S. H., Pan, M., Lin, P., Anghileri, D., Forsythe, N., Pritchard, D. M. W., Fowler, H. J., Obuobie,  
610 E., Darko, D., and Sheffield, J.: Variability and changes in hydrological drought in the Volta Basin, West  
611 Africa, *Journal of Hydrology: Regional Studies*, 42, 101143, <https://doi.org/10.1016/j.ejrh.2022.101143>, 2022c.

612 Gebrechorkos, S. H., Peng, J., Dyer, E., Miralles, D. G., Vicente-Serrano, S. M., Funk, C., Beck, H. E., Asfaw,  
613 D. T., Singer, M. B., and Dadson, S. J.: Global High-Resolution Drought Indices for 1981–2022, *Earth  
614 System Science Data Discussions*, 1–28, <https://doi.org/10.5194/essd-2023-276>, 2023.

615 Geleta, C. D. and Deressa, T. A.: Evaluation of Climate Hazards Group InfraRed Precipitation Station  
616 (CHIRPS) satellite-based rainfall estimates over Finchaa and Neshe Watersheds, Ethiopia, *Engineering Reports*,  
617 3, e12338, <https://doi.org/10.1002/eng2.12338>, 2021.

618 GRDC: The Global Runoff Data Centre, 56068 Koblenz, Germany, 2023.

619 Grogan, D. S., Zuidema, S., Prusevich, A., Wollheim, W. M., Glidden, S., and Lammers, R. B.: Water balance  
620 model (WBM) v.1.0.0: a scalable gridded global hydrologic model with water-tracking functionality,  
621 *Geoscientific Model Development*, 15, 7287–7323, <https://doi.org/10.5194/gmd-15-7287-2022>, 2022.

622 Gu, L., Yin, J., Wang, S., Chen, J., Qin, H., Yan, X., He, S., and Zhao, T.: How well do the multi-satellite and  
623 atmospheric reanalysis products perform in hydrological modelling, *Journal of Hydrology*, 617, 128920,  
624 <https://doi.org/10.1016/j.jhydrol.2022.128920>, 2023.

625 Guo, B., Zhang, J., Xu, T., Croke, B., Jakeman, A., Song, Y., Yang, Q., Lei, X., and Liao, W.: Applicability  
626 Assessment and Uncertainty Analysis of Multi-Precipitation Datasets for the Simulation of Hydrologic Models,  
627 *Water*, 10, 1611, <https://doi.org/10.3390/w10111611>, 2018.

628 Gupta, H. V., Kling, H., Yilmaz, K. K., and Martinez, G. F.: Decomposition of the mean squared error and NSE  
629 performance criteria: Implications for improving hydrological modelling, *Journal of Hydrology*, 377, 80–91,  
630 <https://doi.org/10.1016/j.jhydrol.2009.08.003>, 2009.

631 Hafizi, H. and Sorman, A. A.: Assessment of 13 Gridded Precipitation Datasets for Hydrological Modeling in a  
632 Mountainous Basin, *Atmosphere*, 13, 143, <https://doi.org/10.3390/atmos13010143>, 2022.

633 Harrigan, S., Zsoter, E., Alfieri, L., Prudhomme, C., Salamon, P., Wetterhall, F., Barnard, C., Cloke, H., and  
634 Pappenberger, F.: GloFAS-ERA5 operational global river discharge reanalysis 1979–present, *Earth System  
635 Science Data*, 12, 2043–2060, <https://doi.org/10.5194/essd-12-2043-2020>, 2020.

636 He, Q., Shen, Z., Wan, M., and Li, L.: Precipitable Water Vapor Converted from GNSS-ZTD and ERA5  
637 Datasets for the Monitoring of Tropical Cyclones, *IEEE Access*, 8, 87275–87290,  
638 <https://doi.org/10.1109/ACCESS.2020.2991094>, 2020.

639 Her, Y., Yoo, S.-H., Cho, J., Hwang, S., Jeong, J., and Seong, C.: Uncertainty in hydrological analysis of  
640 climate change: multi-parameter vs. multi-GCM ensemble predictions, *Sci Rep*, 9, 4974,  
641 <https://doi.org/10.1038/s41598-019-41334-7>, 2019.

642 Hersbach, H., Bell, B., Berrisford, P., Hirahara, S., Horányi, A., Muñoz-Sabater, J., Nicolas, J., Peubey, C.,  
643 Radu, R., Schepers, D., Simmons, A., Soci, C., Abdalla, S., Abellan, X., Balsamo, G., Bechtold, P., Biavati, G.,  
644 Bidlot, J., Bonavita, M., De Chiara, G., Dahlgren, P., Dee, D., Diamantakis, M., Dragani, R., Flemming, J.,  
645 Forbes, R., Fuentes, M., Geer, A., Haimberger, L., Healy, S., Hogan, R. J., Hólm, E., Janisková, M., Keeley, S.,  
646 Laloyaux, P., Lopez, P., Lupu, C., Radnoti, G., de Rosnay, P., Rozum, I., Vamborg, F., Villaume, S., and  
647 Thépaut, J.-N.: The ERA5 global reanalysis, *Quarterly Journal of the Royal Meteorological Society*, 146, 1999–  
648 2049, <https://doi.org/10.1002/qj.3803>, 2020.

649 Hong, Y., Xuan Do, H., Kessler, J., Fry, L., Read, L., Rafieei Nasab, A., Gronewold, A. D., Mason, L., and  
650 Anderson, E. J.: Evaluation of gridded precipitation datasets over international basins and large lakes, *Journal of  
651 Hydrology*, 607, 127507, <https://doi.org/10.1016/j.jhydrol.2022.127507>, 2022.

652 Hou, D., Charles, M., Luo, Y., Toth, Z., Zhu, Y., Krzysztofowicz, R., Lin, Y., Xie, P., Seo, D.-J., Pena, M., and  
653 Cui, B.: Climatology-Calibrated Precipitation Analysis at Fine Scales: Statistical Adjustment of Stage IV toward  
654 CPC Gauge-Based Analysis, *Journal of Hydrometeorology*, 15, 2542–2557, [https://doi.org/10.1175/JHM-D-11-  
655 0140.1](https://doi.org/10.1175/JHM-D-11-<br/>
655 0140.1), 2014.

656 Huang, Z., Zhang, Y., Xu, J., Fang, X., and Ma, Z.: Can satellite precipitation estimates capture the magnitude  
657 of extreme rainfall Events?, *Remote Sensing Letters*, 13, 1048–1057,  
658 <https://doi.org/10.1080/2150704X.2022.2123258>, 2022.

659 van Huijgevoort, M. H. J., Hazenberg, P., van Lanen, H. a. J., Teuling, A. J., Clark, D. B., Folwell, S., Gosling,  
660 S. N., Hanasaki, N., Heinke, J., Koirala, S., Stacke, T., Voss, F., Sheffield, J., and Uijlenhoet, R.: Global  
661 Multimodel Analysis of Drought in Runoff for the Second Half of the Twentieth Century, *J. Hydrometeor.*, 14,  
662 1535–1552, <https://doi.org/10.1175/JHM-D-12-0186.1>, 2013.

663 Ibrahim, A. H., Molla, D. D., and Lohani, T. K.: Performance evaluation of satellite-based rainfall estimates for  
664 hydrological modeling over Bilate river basin, Ethiopia, *World Journal of Engineering*, ahead-of-print,  
665 <https://doi.org/10.1108/WJE-03-2022-0106>, 2022.

666 Jiang, Q., Li, W., Wen, J., Fan, Z., Chen, Y., Scaioni, M., and Wang, J.: Evaluation of satellite-based products  
667 for extreme rainfall estimations in the eastern coastal areas of China, *Journal of Integrative Environmental  
668 Sciences*, 16, 191–207, <https://doi.org/10.1080/1943815X.2019.1707233>, 2019.

669 Jiang, S., Wei, L., Ren, L., Zhang, L., Wang, M., and Cui, H.: Evaluation of IMERG, TMPA, ERA5, and CPC  
670 precipitation products over mainland China: Spatiotemporal patterns and extremes, *Water Science and  
671 Engineering*, 16, 45–56, <https://doi.org/10.1016/j.wse.2022.05.001>, 2023.

672 Jiao, D., Xu, N., Yang, F., and Xu, K.: Evaluation of spatial-temporal variation performance of ERA5  
673 precipitation data in China, *Sci Rep*, 11, 17956, <https://doi.org/10.1038/s41598-021-97432-y>, 2021.

674 Kidd, C. and Levizzani, V.: Status of satellite precipitation retrievals, *Hydrology and Earth System Sciences*, 15,  
675 1109–1116, <https://doi.org/10.5194/hess-15-1109-2011>, 2011.

676 Kidd, C., Becker, A., Huffman, G. J., Muller, C. L., Joe, P., Skofronick-Jackson, G., and Kirschbaum, D. B.: So,  
677 How Much of the Earth’s Surface Is Covered by Rain Gauges?, *Bulletin of the American Meteorological  
678 Society*, 98, 69–78, <https://doi.org/10.1175/BAMS-D-14-00283.1>, 2017.

679 Knoben, W. J. M., Freer, J. E., and Woods, R. A.: Technical note: Inherent benchmark or not? Comparing  
680 Nash–Sutcliffe and Kling–Gupta efficiency scores, *Hydrology and Earth System Sciences*, 23, 4323–4331,  
681 <https://doi.org/10.5194/hess-23-4323-2019>, 2019.

682 Laiti, L., Mallucci, S., Piccolroaz, S., Bellin, A., Zardi, D., Fiori, A., Nikulin, G., and Majone, B.: Testing the  
683 Hydrological Coherence of High-Resolution Gridded Precipitation and Temperature Data Sets, *Water Resources  
684 Research*, 54, 1999–2016, <https://doi.org/10.1002/2017WR021633>, 2018.

685 Lakew, H. B.: Investigating the effectiveness of bias correction and merging MSWEP with gauged rainfall for  
686 the hydrological simulation of the upper Blue Nile basin, *Journal of Hydrology: Regional Studies*, 32, 100741,  
687 <https://doi.org/10.1016/j.ejrh.2020.100741>, 2020.

688 Lavers, D. A., Harrigan, S., and Prudhomme, C.: Precipitation Biases in the ECMWF Integrated Forecasting  
689 System, *Journal of Hydrometeorology*, 22, 1187–1198, <https://doi.org/10.1175/JHM-D-20-0308.1>, 2021.

690 Lavers, D. A., Simmons, A., Vamborg, F., and Rodwell, M. J.: An evaluation of ERA5 precipitation for climate  
691 monitoring, *Quarterly Journal of the Royal Meteorological Society*, 148, 3152–3165,  
692 <https://doi.org/10.1002/qj.4351>, 2022.

693 Lehner, B., Verdin, K. L., and Jarvis, A.: New global hydrography derived from spaceborne elevation data, *Eos*,  
694 *Transactions, American Geophysical Union*, 89, 2, <https://doi.org/10.1029/2008EO100001>, 2008.

695 Lehner, B., Liermann, C. R., Revenga, C., Vörösmarty, C., Fekete, B., Crouzet, P., Döll, P., Endejan, M.,  
696 Frenken, K., Magome, J., Nilsson, C., Robertson, J. C., Rödel, R., Sindorf, N., and Wisser, D.: High-resolution  
697 mapping of the world’s reservoirs and dams for sustainable river-flow management, *Frontiers in Ecology and*  
698 *the Environment*, 9, 494–502, <https://doi.org/10.1890/100125>, 2011.

699 Li, L., Wang, Y., Wang, L., Hu, Q., Zhu, Z., Li, L., and Li, C.: Spatio-temporal accuracy evaluation of MSWEP  
700 daily precipitation over the Huaihe River Basin, China: A comparison study with representative satellite- and  
701 reanalysis-based products, *J. Geogr. Sci.*, 32, 2271–2290, <https://doi.org/10.1007/s11442-022-2047-9>, 2022a.

702 Li, M., Lv, X., Zhu, L., Uchenna Ochege, F., and Guo, H.: Evaluation and Application of MSWEP in Drought  
703 Monitoring in Central Asia, *Atmosphere*, 13, 1053, <https://doi.org/10.3390/atmos13071053>, 2022b.

704 Lin, P., Pan, M., Beck, H. E., Yang, Y., Yamazaki, D., Frasson, R., David, C. H., Durand, M., Pavelsky, T. M.,  
705 Allen, G. H., Gleason, C. J., and Wood, E. F.: Global Reconstruction of Naturalized River Flows at 2.94 Million  
706 Reaches, *Water Resources Research*, 55, 6499–6516, <https://doi.org/10.1029/2019WR025287>, 2019.

707 López López, P., Sutanudjaja, E. H., Schellekens, J., Sterk, G., and Bierkens, M. F. P.: Calibration of a large-  
708 scale hydrological model using satellite-based soil moisture and evapotranspiration products, *Hydrology and*  
709 *Earth System Sciences*, 21, 3125–3144, <https://doi.org/10.5194/hess-21-3125-2017>, 2017.

710 Luo, X., Wu, W., He, D., Li, Y., and Ji, X.: Hydrological Simulation Using TRMM and CHIRPS Precipitation  
711 Estimates in the Lower Lancang-Mekong River Basin, *Chin. Geogr. Sci.*, 29, 13–25,  
712 <https://doi.org/10.1007/s11769-019-1014-6>, 2019.

713 Maggioni, V. and Massari, C.: On the performance of satellite precipitation products in riverine flood modeling:  
714 A review, *Journal of Hydrology*, 558, 214–224, <https://doi.org/10.1016/j.jhydrol.2018.01.039>, 2018.

715 Mazzoleni, M., Brandimarte, L., and Amaranto, A.: Evaluating precipitation datasets for large-scale distributed  
716 hydrological modelling, *Journal of Hydrology*, 578, 124076, <https://doi.org/10.1016/j.jhydrol.2019.124076>,  
717 2019.

718 Mehran, A. and AghaKouchak, A.: Capabilities of satellite precipitation datasets to estimate heavy precipitation  
719 rates at different temporal accumulations, *Hydrological Processes*, 28, 2262–2270,  
720 <https://doi.org/10.1002/hyp.9779>, 2014.

721 Menne, M. J., Durre, I., Vose, R. S., Gleason, B. E., and Houston, T. G.: An Overview of the Global Historical  
722 Climatology Network-Daily Database, *Journal of Atmospheric and Oceanic Technology*, 29, 897–910,  
723 <https://doi.org/10.1175/JTECH-D-11-00103.1>, 2012.

724 Mianabadi, A., Salari, K., and Pourmohamad, Y.: Drought monitoring using the long-term CHIRPS  
725 precipitation over Southeastern Iran, *Appl Water Sci*, 12, 183, <https://doi.org/10.1007/s13201-022-01705-4>,  
726 2022.

727 Miao, C., Ashouri, H., Hsu, K.-L., Sorooshian, S., and Duan, Q.: Evaluation of the PERSIANN-CDR Daily  
728 Rainfall Estimates in Capturing the Behavior of Extreme Precipitation Events over China, *Journal of*  
729 *Hydrometeorology*, 16, 1387–1396, <https://doi.org/10.1175/JHM-D-14-0174.1>, 2015.

730 Miao, Q., Pan, B., Wang, H., Hsu, K., and Sorooshian, S.: Improving Monsoon Precipitation Prediction Using  
731 Combined Convolutional and Long Short Term Memory Neural Network, *Water*, 11, 977,  
732 <https://doi.org/10.3390/w11050977>, 2019.

733 Michaelides, S., Levizzani, V., Anagnostou, E., Bauer, P., Kasparis, T., and Lane, J. E.: Precipitation:  
734 Measurement, remote sensing, climatology and modeling, *Atmospheric Research*, 94, 512–533,  
735 <https://doi.org/10.1016/j.atmosres.2009.08.017>, 2009.

736 Moazami, S., Golian, S., Kavianpour, M. R., and Hong, Y.: Comparison of PERSIANN and V7 TRMM Multi-  
737 satellite Precipitation Analysis (TMPA) products with rain gauge data over Iran, *International Journal of Remote*  
738 *Sensing*, 34, 8156–8171, <https://doi.org/10.1080/01431161.2013.833360>, 2013.

739 Moragoda, N. and Cohen, S.: Climate-induced trends in global riverine water discharge and suspended sediment  
740 dynamics in the 21st century, *Global and Planetary Change*, 191, 103199,  
741 <https://doi.org/10.1016/j.gloplacha.2020.103199>, 2020.

742 Nguyen, P., Thorstensen, A., Sorooshian, S., Hsu, K., Aghakouchak, A., Ashouri, H., Tran, H., and Braithwaite,  
743 D.: Global Precipitation Trends across Spatial Scales Using Satellite Observations, *Bulletin of the American*  
744 *Meteorological Society*, 99, 689–697, <https://doi.org/10.1175/BAMS-D-17-0065.1>, 2018.

745 Opere, A. O., Waswa, R., and Mutua, F. M.: Assessing the Impacts of Climate Change on Surface Water  
746 Resources Using WEAP Model in Narok County, Kenya, *Frontiers in Water*, 3, 2022.

747 Palharini, R. S. A., Vila, D. A., Rodrigues, D. T., Quispe, D. P., Palharini, R. C., de Siqueira, R. A., and de  
748 Sousa Afonso, J. M.: Assessment of the Extreme Precipitation by Satellite Estimates over South America,  
749 *Remote Sensing*, 12, 2085, <https://doi.org/10.3390/rs12132085>, 2020.

750 Parker, W. S.: Reanalyses and Observations: What's the Difference?, *Bulletin of the American Meteorological*  
751 *Society*, 97, 1565–1572, <https://doi.org/10.1175/BAMS-D-14-00226.1>, 2016.

752 Peng, J., Dadson, S., Hirpa, F., Dyer, E., Lees, T., Miralles, D. G., Vicente-Serrano, S. M., and Funk, C.: A pan-  
753 African high-resolution drought index dataset, *Earth System Science Data*, 12, 753–769,  
754 <https://doi.org/10.5194/essd-12-753-2020>, 2020.

755 Raimonet, M., Oudin, L., Thieu, V., Silvestre, M., Vautard, R., Rabouille, C., and Moigne, P. L.: Evaluation of  
756 Gridded Meteorological Datasets for Hydrological Modeling, *Journal of Hydrometeorology*, 18, 3027–3041,  
757 <https://doi.org/10.1175/JHM-D-17-0018.1>, 2017.

758 Reichle, R. H., Koster, R. D., Lannoy, G. J. M. D., Forman, B. A., Liu, Q., Mahanama, S. P. P., and Touré, A.:  
759 Assessment and Enhancement of MERRA Land Surface Hydrology Estimates, *Journal of Climate*, 24, 6322–  
760 6338, <https://doi.org/10.1175/JCLI-D-10-05033.1>, 2011.

761 Reis, A. A. dos, Weerts, A., Ramos, M.-H., Wetterhall, F., and Fernandes, W. dos S.: Hydrological data and  
762 modeling to combine and validate precipitation datasets relevant to hydrological applications, *Journal of*  
763 *Hydrology: Regional Studies*, 44, 101200, <https://doi.org/10.1016/j.ejrh.2022.101200>, 2022.

764 Sadeghi, M., Nguyen, P., Naeini, M. R., Hsu, K., Braithwaite, D., and Sorooshian, S.: PERSIANN-CCS-CDR, a  
765 3-hourly 0.04° global precipitation climate data record for heavy precipitation studies, *Sci Data*, 8, 157,  
766 <https://doi.org/10.1038/s41597-021-00940-9>, 2021.

767 Salehi, H., Sadeghi, M., Golian, S., Nguyen, P., Murphy, C., and Sorooshian, S.: The Application of  
768 PERSIANN Family Datasets for Hydrological Modeling, *Remote Sensing*, 14, 3675,  
769 <https://doi.org/10.3390/rs14153675>, 2022.

770 Satgé, F., Ruelland, D., Bonnet, M.-P., Molina, J., and Pillco, R.: Consistency of satellite-based precipitation  
771 products in space and over time compared with gauge observations and snow- hydrological modelling in the  
772 Lake Titicaca region, *Hydrology and Earth System Sciences*, 23, 595–619, [https://doi.org/10.5194/hess-23-595-](https://doi.org/10.5194/hess-23-595-2019)  
773 2019, 2019.

774 Seyyedi, H., Anagnostou, E. N., Beighley, E., and McCollum, J.: Hydrologic evaluation of satellite and  
775 reanalysis precipitation datasets over a mid-latitude basin, *Atmospheric Research*, 164–165, 37–48,  
776 <https://doi.org/10.1016/j.atmosres.2015.03.019>, 2015.

777 Shaowei, N., Jie, W., Juliang, J., Xiaoyan, X., Yuliang, Z., Fan, S., and Linlin, Z.: Comprehensive evaluation of  
778 satellite-derived precipitation products considering spatial distribution difference of daily precipitation over  
779 eastern China, *Journal of Hydrology: Regional Studies*, 44, 101242, <https://doi.org/10.1016/j.ejrh.2022.101242>,  
780 2022.

781 Sheffield, J., Goteti, G., and Wood, E. F.: Development of a 50-Year High-Resolution Global Dataset of  
782 Meteorological Forcings for Land Surface Modeling, *J. Climate*, 19, 3088–3111,  
783 <https://doi.org/10.1175/JCLI3790.1>, 2006.

784 Sheffield, J., Wood, E. F., Pan, M., Beck, H., Coccia, G., Serrat-Capdevila, A., and Verbist, K.: Satellite Remote  
785 Sensing for Water Resources Management: Potential for Supporting Sustainable Development in Data-Poor  
786 Regions, *Water Resources Research*, 54, 9724–9758, <https://doi.org/10.1029/2017WR022437>, 2018.

787 Shen, Y., Xiong, A., Wang, Y., and Xie, P.: Performance of high-resolution satellite precipitation products over  
788 China, *Journal of Geophysical Research: Atmospheres*, 115, <https://doi.org/10.1029/2009JD012097>, 2010.

789 Solakian, J., Maggioni, V., and Godrej, A. N.: On the Performance of Satellite-Based Precipitation Products in  
790 Simulating Streamflow and Water Quality During Hydrometeorological Extremes, *Frontiers in Environmental*  
791 *Science*, 8, 2020.

792 Sun, G., Wei, Y., Wang, G., Shi, R., Chen, H., and Mo, C.: Downscaling Correction and Hydrological  
793 Applicability of the Three Latest High-Resolution Satellite Precipitation Products (GPM, GSMAP, and  
794 MSWEP) in the Pingtang Catchment, China, *Advances in Meteorology*, 2022, e6507109,  
795 <https://doi.org/10.1155/2022/6507109>, 2022.

796 Sun, Q., Miao, C., Duan, Q., Ashouri, H., Sorooshian, S., and Hsu, K.-L.: A Review of Global Precipitation  
797 Data Sets: Data Sources, Estimation, and Intercomparisons, *Reviews of Geophysics*, 56, 79–107,  
798 <https://doi.org/10.1002/2017RG000574>, 2018.

799 Tang, X., Zhang, J., Gao, C., Ruben, G. B., and Wang, G.: Assessing the Uncertainties of Four Precipitation  
800 Products for Swat Modeling in Mekong River Basin, *Remote Sensing*, 11, 304,  
801 <https://doi.org/10.3390/rs11030304>, 2019.

802 Ursulak, J. and Coulbaly, P.: Integration of hydrological models with entropy and multi-objective optimization  
803 based methods for designing specific needs streamflow monitoring networks, *Journal of Hydrology*, 593,  
804 125876, <https://doi.org/10.1016/j.jhydrol.2020.125876>, 2021.

805 Voisin, N., Wood, A. W., and Lettenmaier, D. P.: Evaluation of Precipitation Products for Global Hydrological  
806 Prediction, *Journal of Hydrometeorology*, 9, 388–407, <https://doi.org/10.1175/2007JHM938.1>, 2008.

807 Wang, M., Rezaie-Balf, M., Naganna, S. R., and Yaseen, Z. M.: Sourcing CHIRPS precipitation data for  
808 streamflow forecasting using intrinsic time-scale decomposition based machine learning models, *Hydrological*  
809 *Sciences Journal*, 66, 1437–1456, <https://doi.org/10.1080/02626667.2021.1928138>, 2021.

810 Wang, N., Liu, W., Sun, F., Yao, Z., Wang, H., and Liu, W.: Evaluating satellite-based and reanalysis  
811 precipitation datasets with gauge-observed data and hydrological modeling in the Xihe River Basin, China,  
812 *Atmospheric Research*, 234, 104746, <https://doi.org/10.1016/j.atmosres.2019.104746>, 2020.  
813 Wati, T., Hadi, T. W., Sopaheluwakan, A., and Hutasoit, L. M.: Statistics of the Performance of Gridded  
814 Precipitation Datasets in Indonesia, *Advances in Meteorology*, 2022, e7995761,  
815 <https://doi.org/10.1155/2022/7995761>, 2022.  
816 Wisser, D., Fekete, B. M., Vörösmarty, C. J., and Schumann, A. H.: Reconstructing 20th century global  
817 hydrography: a contribution to the Global Terrestrial Network- Hydrology (GTN-H), *Hydrology and Earth  
818 System Sciences*, 14, 1–24, <https://doi.org/10.5194/hess-14-1-2010>, 2010.  
819 Wollheim, W. M., Vörösmarty, C. J., Bouwman, A. F., Green, P., Harrison, J., Linder, E., Peterson, B. J.,  
820 Seitzinger, S. P., and Syvitski, J. P. M.: Global N removal by freshwater aquatic systems using a spatially  
821 distributed, within-basin approach, *Global Biogeochemical Cycles*, 22, <https://doi.org/10.1029/2007GB002963>,  
822 2008.  
823 Wu, Z., Xu, Z., Wang, F., He, H., Zhou, J., Wu, X., and Liu, Z.: Hydrologic Evaluation of Multi-Source  
824 Satellite Precipitation Products for the Upper Huaihe River Basin, China, *Remote Sensing*, 10, 840,  
825 <https://doi.org/10.3390/rs10060840>, 2018.  
826 Xiang, Y., Chen, J., Li, L., Peng, T., and Yin, Z.: Evaluation of Eight Global Precipitation Datasets in  
827 Hydrological Modeling, *Remote Sensing*, 13, 2831, <https://doi.org/10.3390/rs13142831>, 2021.  
828 Zambrano-Bigiarini, M., Nauditt, A., Birkel, C., Verbist, K., and Ribbe, L.: Temporal and spatial evaluation of  
829 satellite-based rainfall estimates across the complex topographical and climatic gradients of Chile, *Hydrology  
830 and Earth System Sciences Discussions*, 1–43, <https://doi.org/10.5194/hess-2016-453>, 2016.  
831 Zhu, D., Ilyas, A. M., Wang, G., and Zeng, B.: Long-term hydrological assessment of remote sensing  
832 precipitation from multiple sources over the lower Yangtze River basin, China, *Meteorological Applications*, 28,  
833 e1991, <https://doi.org/10.1002/met.1991>, 2021.  
834 Zhu, H., Li, Y., Huang, Y., Li, Y., Hou, C., and Shi, X.: Evaluation and hydrological application of satellite-  
835 based precipitation datasets in driving hydrological models over the Huifan river basin in Northeast China,  
836 *Atmospheric Research*, 207, 28–41, <https://doi.org/10.1016/j.atmosres.2018.02.022>, 2018.  
837